d·Collection

Ph.D. Dissertation

Finite Element Model Updating of Multi-girder Bridges Considering Relative Girder Displacement

거더의 상대 변위를 고려한 다중 거더 교량의
유한요소 모델 개선

August 2017

Graduate School of Engineering
Seoul National University
Department of Civil and Environmental Engineering

Dobeen Kim

Abstract

Bridge in operation experiences deteriorations due to various factors such as aging and damages, and the structural performance of a bridge thus changes continuously over its lifetime. For safe operation and cost-effective maintenance of the bridge, precise evaluation of current performance of the bridge is essential. Recently as an index of the performance of bridge, Load Rating Factor (RF) is regarded as quantitative and objective in comparison with other typically-used methods. RF is usually calculated by finite element (FE) analysis in which a baseline FE model needs to be updated using field measurement which can portray the actual structural behavior. Generally, load testing is conducted in order to update FE model. On the other hand, FE models can also be updated using an ambient vibration data without performing costly load testing. However, But it has a limitation that individual stiffness information of each member or local level, which can affect greatly the accuracy of RF, is difficult to be attained.

This study proposes a new finite element model updating method using ambient vibration data which can enhance the accuracy of updated FE model by adapting Relative Girder Displacement (RGD) and Relative Girder Displacement Accuracy Criterion (RGDAC) concepts. RGD and RGDAC can be regarded as a supplementation to each other because RGD is defined as individual values while RGDAC represents shape with a vector. The two indices are embedded into objective function of optimization in FE model updating procedure, and optimal form of an objective function with RGD and RGDAC is obtained from various numerical

simulations. In order to verify the proposed method, a simulated bridge model is created based on an existing bridge. FE model is updated according to proposed method in order that its response becomes closer to that of simulated bridge model. The updated model shows good agreement with simulated bridge model with assumed stiffness deterioration. The generality of the proposed method is confirmed by verifying the results for the cases under various lane load locations. As an illustrative example, FE model for an actual existing bridge is composed and updated by using dynamic displacement data. With the updated FE model, RF is calculated to confirm the proposed method and show its practical application.

.

Keywords: Finite Element Model Update, Ambient Vibration Data, Relative Girder Displacement (RGD), Relative Girder Displacement Assurance Criterion (RGDAC)

Student Number: 2011-23392

Table of Contents

List of Figures

VIII

List of Tables

Chapter 1. Introduction

This chapter describes the background of the research and provides a literature review of finite element model update methods that incorporate measurement data. The research objectives and the scope of the research are summarized along with an overview of the dissertation.

1.1 Research Background

The actual structural performance of a bridge may be inferior to the performance required by the design specifications when extreme events induce structural damage or when structural deterioration occurs during the lifetime of the bridge. Various approaches have therefore been developed to assess structural conditions using empirical and analytical methods such as visual inspection, nondestructive testing, and field testing to determine the bridge's structural safety. However, visual inspection by a human evaluator could produce subjective assessment results, and if access to certain structural members is limited, the inspection results cannot be accepted with a high level of confidence.

To address this issue, a method has been developed to evaluate load rating factors using a finite element model that is updated based on current structural behavior observed in field tests. In general, field tests are initially performed to obtain specific structural responses including displacement, strain, natural frequency, and mode shape under known load conditions; the finite element model is then updated through an optimization process that involves determination of structural

parameters that give similar structural responses under the same load conditions. However, this method requires traffic control for the bridge to be in operation and thus would entail high social and economic costs. Because of this difficulty, finite element model update methods based on ambient vibration tests were proposed to identify the natural frequency and mode shape characteristics. Dynamic data are generally more suitable for identification of global structural behavior than static data. Additionally, when compared with static measurement data, dynamic data can be obtained without the requirement for traffic control and continuous measurement activity could be maintained over longer periods using permanently installed sensors. However, dynamic data, which represent the global response using the natural frequency, the mode shape, and the damping ratio, are less sensitive to changes in the local structural parameters, which greatly affect the evaluation of the load rating factor.

1.2 Literature Survey

Structural inspection can provide meaningful results when structural damage such as cracking, stalls, chemical deterioration or corrosion is noticeable. In general, however, there is a lack of correlation between the visual appearance and actual structural reliability (Catbas, 2002). Therefore, a great deal of research has been carried out to combine finite element analysis processes with measurement data for the purposes of bridge evaluation (Schlune, 2009). When the evaluation of the structural deterioration of a bridge by analytical methods is questionable, a field testing method such as diagnostic testing or proof testing is the most appropriate

approach to provide an understanding of the current structural performance. In particular, safety verification of a bridge that is in operation is often addressed by either analysis or load testing. When compared with analysis methods, load testing represents a much more economical method, and it is particularly essential when the evaluator feels that analytical approaches do not represent the actual structural behavior correctly or when there is a lack of the information that is required for the analytical methods. Therefore, field testing and monitoring methods for improvement of the structural models used for bridge assessment have also been investigated (Cruz, 2006).

The procedure of updating a finite element model using measurement data is effectively an optimization problem that involves determination of the most appropriate structural parameters (Park, 2012). Various types of measurement data are generally required to update finite element models (Catbas, 2007). Strain measurements taken under truck loading conditions have been used to determine the support constraints and the cross-sectional properties of steel girder and concrete slab bridges (Chajes et al., 1997). Strain and displacement measurements have also been used to improve the accuracy of finite element models (Huang, 2004). In addition to static or quasi-static load testing, modal characteristics have also been used extensively to obtain additional information about the bridge's responses (Daniell, 2007).

The issue of the measurement data variability when performing model updates has also been studied (Robert-Nicoud et al., 2000; Schuëller et al., 2008). The long-term effects of deformation reactions can be ignored in short-term field experiments such as traffic load tests. This type of test is usually completed in a short period of

time and records only short-term structural behavior. In contrast, long-term continuous monitoring can capture real-time structural behavior that cannot be observed easily in short-term tests, such as daily and seasonal behavioral fluctuations (Cardini and DeWolf 2008). From this perspective, ambient vibration testing and long-term monitoring processes have been performed to support the assessment of bridge structures (Catbas et al. 2013; Grimmelsman, 2006; Zhang et al. 2013; He et al. 2009). Long-term monitoring processes commonly provide strain and acceleration responses (Doebling et al. 1998; Chang 2002; Mufti and Bakht 2002).

1.3 Research Objectives and Scope

This study proposes a new method for evaluation of structural performance based on updating of a finite element model. Measurement data are used to estimate the stiffness of the bridge structure through the proposed model update process. The finite element model is updated by performing optimization processes based on the measurement data. The objective function consists of the natural frequencies of the structure, the relative girder displacement (RGD) and the relative girder displacement assurance criterion (RGDAC). The RGD is defined by the static displacement or the dynamic displacement on each girder. The RGDAC describes the degree of consistency between the measured RGD and the RGD from analysis using a real-valued scalar such as a modal assurance criterion (MAC) (Allemang, 2002). The sensitivity of the structural parameters is also investigated via a global sensitivity analysis. A genetic algorithm is used to update the finite element model, and the validity of the results of the update is examined through a study of the

convergence conditions. The updated finite element model is then regarded as a structural model that describes the structural behavior in a similar manner to the measurement data. Consequently, the structural parameters of the updated finite element model represent the actual condition of the bridge structure.

The proposed method is demonstrated using numerical examples of a simulated bridge model and the Yeondae Bridge in Korea. The validity of the proposed method is then checked by comparing the analytical predictions of the updated finite element model with measured data such as the displacement, the natural frequency, and the mode shape using the simulated numerical example. In addition, because a simulated bridge model has the advantage of knowing the structural parameter values, which are unknown values in the case of a real bridge structure, the effects of updating the stiffness using the proposed method are confirmed by comparing the true structural parameter values with the updated structural parameters. In the simulated bridge model, the proposed method assumes cases where the flexural stiffness of one inner girder is particularly low and where the flexural stiffness values of some of the inner girders and outer girders are similarly low. Finally, the flexural stiffness of the girder is selected randomly using a uniform probabilistic distribution based on the baseline finite element model. In addition, the proposed approach is tested using the real structure of the Yeondae Bridge. The effectiveness of the proposed method is demonstrated by comparing the values from the structural analysis with the evaluated load rating.

1.4 Overview of Dissertation

This dissertation consists of five chapters. Chapter 1 provides the research background, a literature review, the research objectives and scope, and an overview of the dissertation. Chapter 2 presents the method used to update the finite element model using the dynamic response and describes the mathematical issues associated with this method. The relative girder displacement (RGD) is used to update the structural parameters of the finite element model. Unlike the static displacement, which is the exact structural response to an applied load, the RGD can provide the relative stiffness of the structure. The relative girder displacement assurance criterion (RGDAC) is proposed to assure a degree of consistency between the measured RGD and the RGD from the analysis in a real scalar value. Chapter 3 presents numerical verification through application of the proposed method to an example of a simulated bridge model that was developed based on the New Jersey Bridge. In addition, to generalize the proposed method, the method is applied in the cases where the flexural stiffness of an inner girder is particularly low, where the flexural stiffness values of some of the inner and outer girders are similarly low, and where the flexural stiffness of a girder is irregular. The effect of updating the finite element model was confirmed by comparing the structural response and the evaluation of the load rating with simulated true values. Chapter 4 describes a numerical example in which the proposed method is applied to the Yeondae Bridge. The effect of updating the finite element model was confirmed by comparing the structural response and the evaluation of the load rating with simulated true values. Chapter 5 summarizes the results of this study and suggests subjects for future study.

Chapter 2. Finite Element Model Updating using Relative Girder Displacement

The relative girder displacement (RGD) is used to update the structural variables of the finite element model. The RGD can provide the relative stiffness of the structure. However, minimization of the discrepancy between the measured RGD and the RGD obtained from analysis using the finite element model may provide a different stiffness distribution because the RGD has different properties to those of the static displacement, which is the exact structural response to an applied load. The relative girder displacement assurance criterion (RGDAC) is intended to ensure a degree of consistency between the measured RGD and the RGD from analysis in terms of a real scalar value. The RGDAC takes values ranging from zero, which represents an inconsistent correspondence, to one, which represents a consistent correspondence. The RGD and the RGDAC supplement each other for a limitation of the relative displacement of the girder during the process of updating the finite element model.

2.1 Relative Girder Displacement of Multi-girder Bridges

2.1.1 Advantage of using the Relative Girder Displacement for Finite Element Model Updating

Safety verification of an occupied bridge is conducted by processes of analysis and/or load testing. When compared with analysis-based methods, load testing is a more costly method, but has been accepted as an essential method when the surveyor feels that analytical approaches do not represent the actual structural behavior of the

bridge or do not produce sufficient information. In relation to this, field testing and monitoring methods for improvement of the structural models used for bridge assessment have been studied (Cruz, 2006). When structural deterioration of the bridge may lead to uncertain variables for use in the analytical methods, field testing methods such as diagnostic testing and proof testing represent the appropriate approach required to understand the bridge's current structural performance. There are two types of measurement data: static and dynamic. In general, different types of measurement data are required to update the finite element model (Catbas, 2007).

The main advantage of static data is that these data can be used to retrieve an exact value at an exact location, whereas dynamic data cannot be used to determine a value at an exact location because of vibrations. In other words, the output data from static testing are clearer than those from dynamic testing. Therefore, static data provide more accurate information to update the finite element model. Additionally, when the purpose of updating the finite element model is to evaluate a local structural member, static data are better suited to determination of the local parameters. However, the problem with static tests is that they require traffic control and traffic control on bridges that are in public use is not a simple task. For example, load testing may be impractical because of test access difficulties or site traffic conditions.

In contrast, dynamic data are suitable for determination of global structural behavior because these data contain information about the global response of the structure. When compared with data from static measurements, dynamic data can be obtained without the need for traffic control and continuous measurement activities can be observed over longer periods using permanently installed sensors. However, dynamic data, which include global responses such as the natural frequency, the

mode shape, and the damping ratio, are less sensitive to local structural parameters. Therefore, to obtain data with high levels of accuracy, a dense network of sensors is required.

Measurements of the vertical displacement of girders that occurs when a vertical load acts on a bridge structure can be obtained from both dynamic and static loading tests. The static displacement of the girder is useful when updating the stiffness of the girder used in the baseline finite element model. The static displacement of the measured girder is known precisely based on the position and the magnitude of the load, whereas the dynamic displacement of the girder obtained from ambient vibration testing or moving vehicle testing cannot be used determine the exact magnitude and position of the applied load. Therefore, the measured dynamic girder displacement is too complex to be used to update the finite element model.

However, the RGD is dependent on the position of the load and shows similar values for different loads at the same position, regardless of the magnitude of the load. The RGD also offers the advantage that it can be obtained from both static and dynamic loading tests. In this study, the finite element model is therefore updated using RGD values obtained from both static and dynamic loading tests.

2.1.2 Definition of Relative Girder Displacement

In order to define the relative girder displacement, it is first necessary to define the vertical displacement of each girder.
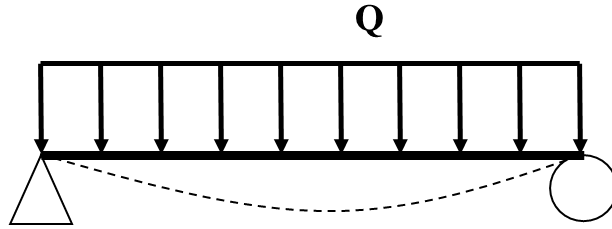
Figure 2. 1 Example of girder displacement by applied load (Q)

In general, any type of load (Q) can cause the vertical displacement of a girder, including concentrated loads, distributed loads, and moment loads. In this research, only the lane load is considered for convenience. In addition, a representative displacement quantity is required for each girder. The vertical displacement at the mid-span point of the girder is considered to be the most appropriate representative value because the maximum displacement response is likely to occur at the center of the girder when measured along the longitudinal direction. The vertical displacement at the center of the i-th girder can therefore be expressed as follows in Eq. (2.1):

$$\delta_i = y_i \left(x = \frac{L_i}{2}, Q_j \right) \qquad (2.1)$$

where Q_j (j=1~number of lanes) is the location of the j-th lane, and $L_i (i = 1$~number of girders$)$ is the span length of the i-th girder. This girder displacement is then used to define the RGD indices that are used to update the finite element models of multi-girder bridges.

2.1.3 Acquisition of the Relative Girder Displacement from Measurement Data

The static displacement is a measure of the value of the vertical displacement when the vehicle is in a specified position on the bridge. It is important is to separate the effect of the vehicle from the measured data until the vehicle reaches the specified

position and the vibration from the vehicle has started. The measured values from the static vehicle loading experiments are then extracted using the average value of the data.

When compared with the static displacement, dynamic displacements represent the superposition of signals at various frequencies, and thus measured dynamic displacements have low-frequency components, which are displacements caused by moving loads, and high-frequency components, which are affected by the interactions between the bridge and the vehicle. Separation of the various frequency signals can be achieved using low-pass filtering, which can eliminate the high-frequency signals so that only the low-frequency components remain. The resulting signals are expected to represent the pseudo-static displacements induced by the truck weight loading (Koh, 2014). The peak values of the filtered displacements can be regarded as static displacements, although the absolute magnitude of the maximum displacement is not exactly the same as the static displacement.
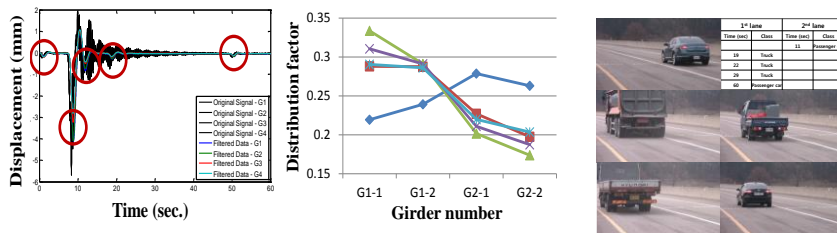
Figure 2. 2 Example of the measured dynamic displacement (Korea Concrete Institute [KCI], 2012)

11

2.2 Relative Girder Displacement Index for Updating Finite Element Model

2.2.1 Relative Girder Displacement Index

In this section, the RGD indices of a multi-girder bridge are defined for use in the finite element model update problem. Consider the eight-girder bridge structure shown in Fig. 2.3.
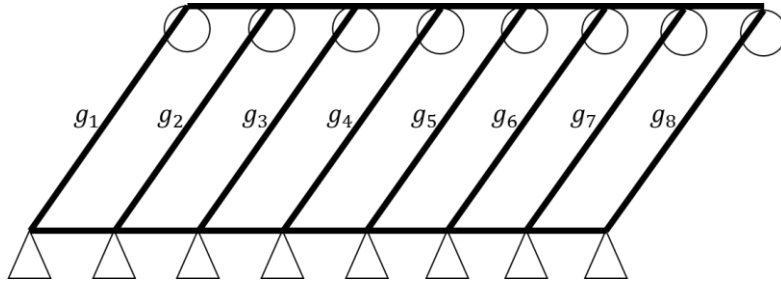
Figure 2. 3 Example of bridge structure

As shown in Fig. 2.3, the vertical displacement δ_i can be determined for each girder for a load Q. Then, the RGD of the i-th girder displacement can be defined as follows.

First, $RGD_{i,sum}$, which is the ratio of the i-th girder displacement to the sum of all girder displacements is given by Eq. (2.2):

$$RGD_{i,sum} = \frac{\delta_i}{\sum_{i=1}^{N} \delta_i} \tag{2.2}$$

where δ_i (i=1~number of girders) is the displacement at each girder. When compared with $RGD_{i,sum}$, $RGD_{i,max}$ shows a higher RGD scalar value. $RGD_{i,max}$ is given by Eq. (2.3):

$$RGD_{i,max} = \frac{\delta_i^D}{\max(\delta_D)} \tag{2.3}$$

where δ_i^D (i=1~number of girders) is the same displacement as shown above, but the ratio in this case is of the maximum load effect among the members (rather than that of a system of girders) to the load effect in a single member, and thus provides a higher RGD scalar value. In general, the purpose of updating the finite element model is to determine the structural parameters that minimize the discrepancies between the measured data and the results obtained from analysis using the finite element model. In this case, $RGD_{i,max}$ would provide more mathematical meaning for the optimization problem. Table 2.1 below shows an example of the discrepancies between $RGD_{i,sum}$ and $RGD_{i,max}$ with regard to interpretation of the dynamic displacement.
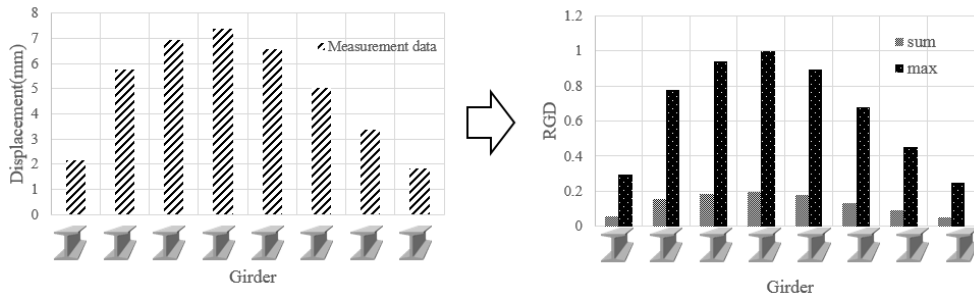
Figure 2. 4 Example of conversion of measured displacements to RGD by interpretation

Table 2. 1 Example showing discrepancies between $RGD_{i,sum}$ and $RGD_{i,max}$

	δ_D(mm)	$RGD_{i,sum}$	$RGD_{i,max}$
1st girder	1.9807	0.0582	0.2928
2nd girder	5.1251	0.1544	0.7768
3rd girder	6.234	0.1867	0.9355
4th girder	6.6449	0.1987	1
5th girder	5.8666	0.1771	0.8913
6th girder	4.3722	0.1348	0.6785
7th girder	2.8536	0.0901	0.4533
8th girder	1.4787	0.0488	0.2457

In addition, only the measured dynamic displacements required to identify the load case are used in cases where the operational monitoring data are used. Various RGD values from the monitoring data should then be clustered to provide structurally meaningful information with which the finite element model can be updated. The "K-means clustering" procedure classifies based on the sum of the distances between data points. The distance from each data point is given by Eq. (2.4):

$$J = \sum_{n=1}^{N} \sum_{k=1}^{k} r_{nk} \|x_n - \mu_k\|^2 \qquad (2.4)$$

where x_n is the data point and μ_k is the centroid mean vector of the k-th cluster. If the data point x_n is placed under the category of k, then $r_{nk} = 1$ and $r_{nk} = 0$ when $j \neq k$. The algorithm iteratively finds the appropriate elements and the centroids of clusters that best minimize the objective function. In this problem, all data points x_n correspond to RGD values.
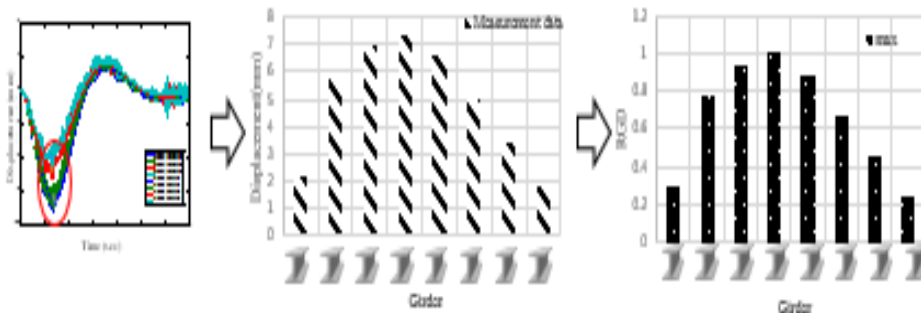
Figure 2. 5 Example of conversion of measured dynamic displacement to RGD (KCI, 2012)

2.2.2 Relative Girder Displacement Assurance Criterion

The relative girder displacement assurance criterion (RGDAC) represents the degree of consistency between the measured RGD and the RGD from analysis in a real-valued scalar such as a modal assurance criterion (MAC). The RGDAC takes values ranging from zero, which represents no consistent correspondence, to one, which represents consistent correspondence. The RGD and the RGDAC supplement each other to limit the dynamic displacement during the process of updating the finite element model. The RGDAC provides the degree of consistency for two vectors in the form of a scalar value. The RGDAC is given by Eq. (2.5):

$$RGDAC = \frac{\left((\overline{RGD_a})^T(\overline{RGD_m})\right)^2}{((\overline{RGD_a})^T(\overline{RGD_a}))((\overline{RGD_m})^T(\overline{RGD_m}))} \tag{2.5}$$

where $\overline{RGD_a}$ and $\overline{RGD_m}$ are the column vectors of the RGD and the subscripts a and m represent the values from analysis of the finite element model and from the measured data, respectively. In addition, $\overline{RGD_a}^T$ and $\overline{RGD_m}^T$ are the corresponding transpose vectors used to represent the degree of consistency for two vectors in the form of a scalar value, respectively.

2.3 Formulation of the Finite Element Model Updating using Relative Girder Displacement Indices

In this research, the error functions for the RGD and the RGDAC when formulated as mathematical expressions are similar to the error functions of the latest research in the field. In general, the design variables in the optimization problem that minimize the differences between the measured structural response and the response

from the finite element model can be varied according to the error function that indicates the differences in the measurements. Therefore, the error functions that represent the differences between the measured response of the structure and the response from the finite element model have been actively studied. This research proposes an objective function consisting of the natural frequencies, the RGD, and the RGDAC for use in updating the finite element model. Additionally, each error function formulates regularization processes for a single objective function and provides higher weight for a higher residual error solution.

2.3.1 Error Function for Value of Modal and Static Displacement

Lee and Cho used the finite element model update method to estimate the fatigue life of a 38.8m short span plate girder bridge and used the optimization method to minimize the objective function. (Lee and Cho 2016) Respectively, the error function for objective function is given by Eq. (2.6)

$$J = \sum_{k=1}^{N} \left\{ w_k \left(\frac{f_k^a - f_k^m}{f_k^m} \right) \right\}^2 \qquad (2.6)$$

where f_k^a and f_k^m are the natural frequencies from analysis and measurements, respectively, and w_k is the k-th weight function for the different natural frequency modes.

In addition, Shabbir and Omenzetter minimized the frequency and mode shape errors when updating a finite element model for a 59.5-m-span steel-reinforced cable-stayed bridge that was constructed as a pedestrian bridge (Shabbir and Omenzetter, 2015). The error function for the objective function is given by Eq. (2.7):

$$J = \sum_{k=1}^{N} \alpha_k \left(\frac{f_k^a - f_k^m}{f_k} \right)^2 + \sum_{k=1}^{N} \beta_k \frac{\left(1 - \sqrt{MAC_k}\right)^2}{MAC_k} \tag{2.7}$$

where f_k^a and f_k^m are natural frequencies of analysis and measured respectively, α_k and β_k are k-th weight function for different natural frequency mode and mode shape respectively. Modal Assurance Criterion (MAC) used to verify mode shape and MAC is given by Eq. (2.8)

$$MAC_k = \frac{\left(\left(\overline{\varphi_k^a}\right)^T \left(\overline{\varphi_k^m}\right) \right)^2}{\left(\left(\overline{\varphi_k^a}\right)^T \left(\overline{\varphi_k^a}\right) \right) \left(\left(\varphi_k^m\right)^T \left(\varphi_k^m\right) \right)} \tag{2.8}$$

The objective function of the optimization problem that must be solved to determine the structural parameters required to produce similar structural behavior in both the values obtained from the finite element model analysis and the measured data should be constructed with the purpose of updating the finite element model with these structural parameters. The objective function for optimization should be able to represent the differences between the measurement data and the structural analysis values numerically so that the error function is defined based on the structural response characteristics. To construct a single objective function for optimization, the error functions for the various structural responses should be averaged such that they affect the objective function values at the same rate, and should also be configured for the purpose of updating the finite element model (Neuman and Yakowitz, 1979; Becks and Murio, 1984; Schnur and Zabaras 1990; Lee *et al*., 1999).

In this study, the error functions for the natural frequency, the vertical displacement, and the mode shape are defined as shown below and follow the latest

mathematical expressions used in this field. In addition, to construct a single objective function, the error functions are defined as shown in Eq. (2.9), Eq. (2.10), and Eq. (2.11), where each error function is given the same ratio weight.

$$e(x)_f = \frac{1}{N}\sum_{j=1}^{N}\left(\frac{f(x)_j^a - f_j^m}{f_j^m}\right)^2 \qquad (2.9)$$

$$e(x)_\delta = \frac{1}{M}\sum_{i=1}^{M}\left(\frac{\delta(x)_i^a - \delta_i^m}{\delta_i^m}\right)^2 \qquad (2.10)$$

$$e(x)_{MAC} = \frac{1}{N}\sum_{j=1}^{N}\frac{\left(1-\sqrt{MAC_j}\right)^2}{MAC_j} \qquad (2.11)$$

where $e(x)_f$ is the residual error of the natural frequency, f_j is the j-th natural frequency (where $j=1$ – number of natural frequencies), $e(x)_\delta$ is the residual error of the static displacement, δ_i is the i-th girder vertical displacement (where $i=1$ ~number of girders), and $e(x)_{MAC}$ is the residual error of the mode shape. The MAC is the modal assurance criterion given in Eq. (2.8), which provides linear consistency for the eigenvector (Randal, 2003). MAC_j is the j-th mode shape (where $j=1$~number of mode shapes). As before, the superscripts a and m represent the values from analysis of the finite element model and the measured data, respectively.

2.3.2 Error Function of the Relative Girder Displacement

In this research, the RGD is defined using the form $RGD_{i,max}$ because it can provide larger discrepancy values during the process of solving the optimization problem, which involves minimization of the residual errors between the measured data and the values obtained from analysis of the finite element model. The error function for the RGD is given by Eq. (2.12) below, following similar expressions for the natural

frequencies and the static displacement. When the girder displacement δ_i (where i=1~number of girders) is defined as described in Chapter 2.1.2, then $RGD_{i,\max}$ is given by Eq. (2.3). The discrepancy between the RGD from measured data and that obtained from analysis can then be determined using Eq. (2.12):

$$e(x)_{RGD} = \frac{1}{M}\sum_{i=1}^{M}\left(\frac{RGD(x)_i^a - RGD_i^m}{RGD_i^m}\right)^2 \tag{2.12}$$

where $e(x)_{RGD}$ is the residual error of the RGD. $RGD(x)_j$ is the RGD of the j-th girder (where j=1~number of girders), and the superscripts a and m represent the values from analysis of the finite element model and from the measured data, respectively.

However, minimization of the discrepancy between the measured RGD and the RGD from analysis of the finite element model may provide different stiffness distributions because the RGD provides a relative ratio only, unlike the static displacement, which is a structural response to an applied load.

2.3.3 Error Function of the Relative Girder Displacement Assurance Criterion

The error function for the RGDAC is equated as Eq. (2.13)

$$e(x)_{RGDAC} = \frac{\left(1 - \sqrt{RGDAC}\right)^2}{RGDAC} \tag{2.13}$$

where $\overline{RGD_a}$ and $\overline{RGD_m}$ are the column vectors of the RGD and the subscripts a and m represent the values from analysis of the finite element model and from the measured data, respectively. In addition, $\overline{RGD_a}^T$ and $\overline{RGD_m}^T$ are the corresponding transpose vectors that represent the degree of consistency for the two

vectors in terms of a scalar value. The RGDAC takes values ranging from zero, which represents no consistent correspondence, to one, which represents consistent correspondence.

Each error function is represented by a numerical nonlinear expression such that it will have a higher weight for larger discrepancies and a lower weight for small discrepancies. As shown in Fig. 2.6, different residual error terms for the RGDAC provide different numerical values within the same RGDAC numerical error range. Residual error term 1 is represented by the linear numerical expression given by Eq. (2.13) and residual error term 2 is represented by the nonlinear numerical expression given by Eq (2.14).

$$e2(x)_{RGDAC} = |1 - RGDAC| \qquad (2.14)$$
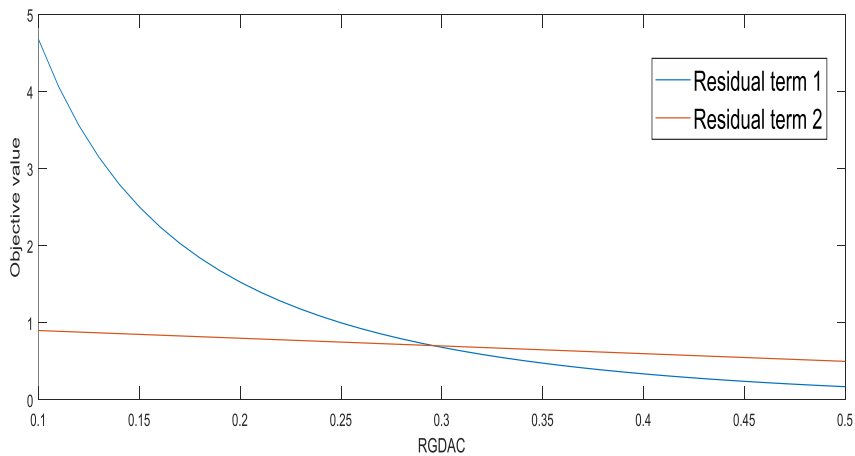
Figure 2. 6 Different error value in terms of numerical expression

2.3.4 Objective Function for Updating Finite Element Model

An optimization problem can be stated as shown in Eq. (2.15), which is subject to inequality and equality constraints.

$$\text{Find X} = \begin{Bmatrix} x_1 \\ x_2 \\ \vdots \\ x_n \end{Bmatrix} \text{ which minimized } f(X) \qquad (2.15)$$

The formulation of the objective function $f(X)$ that is used to update the baseline finite element model has various methods to represent the discrepancies between the measured data and the values from analysis of the finite element model, where x represents the structural parameters. Correct formulation of the objective function used to update the finite element model is essential because it could otherwise provide different update results. In this research, the objective function is formulated to establish the validity of the proposed method.

First, the objective function is constructed by taking the error functions of the natural frequency and the mode shape into consideration and considering the case where only dynamic measurement data can be obtained, giving the function shown in Eq. (2.16).

$$min \, J_1(x) = e(x)_f + e(x)_{MAC} \qquad (2.16)$$

Second, the objective function is constructed by taking the error functions of the natural frequency and the static displacement into consideration while considering the case where only dynamic measurement data and static measurement data can be obtained, giving the function shown in Eq. (2.17).

$$min \, J_2(x) = e(x)_f + e(x)_{MAC} + e(x)_\delta \qquad (2.17)$$

Third, the objective function is constructed by taking the error functions of the natural frequency and the RGD into consideration while considering the case where

only dynamic measurement data and RGD data can be obtained, giving the function shown in Eq. (2.18).

$$min\, J_3(x) = e(x)_f + e(x)_{RGD} \tag{2.18}$$

Fourth, the objective function is constructed by taking the error functions of the natural frequency and the RGDAC into consideration and considering the case where only dynamic measurement data and RGD data can be obtained, giving the function shown in Eq. (2.19).

$$min\, J_4(x) = e(x)_f + e(x)_{RGDAC} \tag{2.19}$$

Finally, the objective function is constructed by taking the error functions of the natural frequency, the RGD, and the RGDAC into consideration and considering the case where only dynamic measurement data and RGD data can be obtained, giving the function shown in Eq. (2.20).

$$min\, J_5(x) = e(x)_f + e(x)_{RGD} + e(x)_{RGDAC} \tag{2.20}$$

2.3.5 Illustrative Example: Error Function of the Relative Girder Displacement

Unlike the static displacement, the RGD represents a relative ratio. Therefore, minimization of the discrepancy between the measured RGD and the RGD from analysis or the discrepancy between the measured RGDAC and the RGDAC from analysis may provide different updates for the finite element model within the same mathematical residual error range. Therefore, the RGD and RGDAC supplement each other in limiting the dynamic displacement during the process of updating the

finite element model. This chapter provides an illustrative example of the limitations of using the RGD or the RGDAC alone.

An idealized numerical example is considered to verify the limitations of updating the finite element model when using only the RGD. The virtual finite element model consists of a simply supported composite reinforced concrete (RC) slab on steel girders. From the virtual dynamic displacement data obtained, $RGD_{i,\max}$ is then determined using Eq. (2.3).
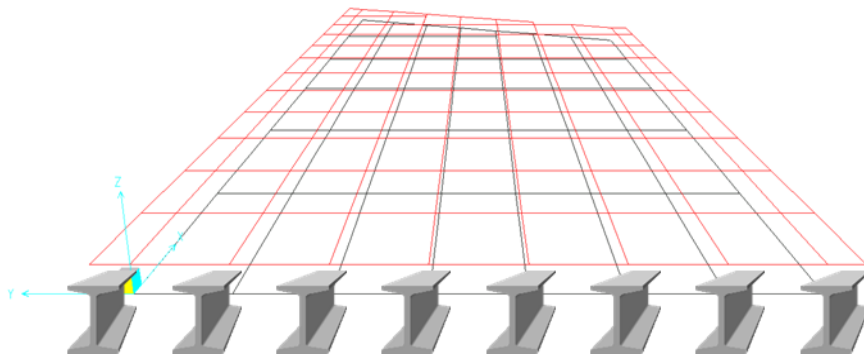
Figure 2. 7 A simulated bridge model for illustrative example

Table 2. 2 Generated simulated measured displacement and RGD

	δ_D(mm)	$RGD_{i,max}$
1st girdier	1.9807	0.2928
2nd girder	5.1251	0.7768
3rd girder	6.234	0.9395
4th girder	6.6449	1
5th girder	5.8666	0.8913
6th girder	4.3722	0.6785
7th girder	2.8536	0.4533
8th girder	1.4787	0.2457

To verify the limitations of updating the finite element model when using only the RGD, the objective function is formulated while considering two types of

residual errors, which are those of the natural frequency and the RGD. The formulated objective function is given as Eq. (2.19):

$$J(x) = e(x)_{\text{RGD}} \tag{2.19}$$

while the residual RGD error is given by Eq. (2.20):

$$e(x)_{\text{RGD}} = \frac{1}{M} \sum_{i=1}^{M} \left(\frac{RGD(x)_j^a - RGD_j^m}{RGD_j^m} \right)^2 = 0.045 \tag{2.20}$$

Figure 2. 8 Measured RGD and updated RGD

Table 2. 3 RGD at each girder

	True RGD	Updated 1	Updated 2	Updated 3
1st girdier	0.2928	0.2928	0.205	0.2308
2nd girder	0.7768	0.7768	0.5438	0.6121
3rd girder	0.9395	0.9395	0.6576	0.7403
4th girder	1	1	1	0.788
5th girder	0.8913	0.6239	0.6239	1
6th girder	0.6785	0.475	0.6785	0.8821
7th girder	0.4533	0.3173	0.4533	0.544
8th girder	0.2457	0.172	0.2457	0.2948

In general, the updated finite element model represents the minimized objective function value, but in this illustrative example, virtual updates are made to

the finite element model to illustrate the limitations of using the RGD only. Updated finite element model cases 1 and 2 show several RGDs that are the same as the corresponding measured RGDs, while several other RGDs still have residual error values. However, updated finite element model 3 shows the wrong location for the member with the maximum RGD, and every RGD at every girder member has a residual error, but smaller residual error values than those of updated finite element models 1 and 2. As shown above, the updated finite element models in cases 1, 2, and 3 show different solutions. However, these solutions have the same residual error values.

The procedure of updating the finite element (FE) model using measurement data is intended to solve the optimization problem by finding the most appropriate structural parameters (Park, 2012). In fact, updating of the FE model is an ill-posed inverse problem, and the uniqueness of the solution is not assured. In other words, various solutions could exist when the FE model is updated. Unlike the static displacement case, the RGD represents a relative ratio. Therefore, minimization of the discrepancy between the measured RGD and the RGD from analysis provides a limitation when updating the FE model to ensure that the relationship between mathematical and physical completeness is maintained. While updated cases 1, 2, and 3 above all show the same residual error value (0.045), they all provide different RGDAC values, which are determined using Eq. (2.13).

Table 2. 4 Scalar value of RGDAC

	Updated case 1	Updated case 2	Updated case 3
RGDAC	0.9741	0.9689	0.9565

As shown in Table 2.4, the RGDAC can provide additional information for use when updating the FE model because the RGDAC provides a degree of consistency for two vectors in the form of a scalar value.

2.3.6 Illustrative Example: Error Function of the Relative Girder Displacement Assurance Criterion

An idealized numerical example is considered here to verify the limitations of using the RGDAC alone to update the FE model. The simulated bridge model again consists of a simply supported composite RC slab on steel girders, as shown in Fig. 2.7. The formulated objective function is given as Eq. (2.21):

$$J(x) = e(x)_{\text{RGDAC}} \tag{2.21}$$

where $e(x)_{RGDAC}$ is given by Eq. (2.13). The RGDAC can only indicate consistency and cannot confirm validity. Even in the case where the MAC value is unity, the RGD or the displacement could represent different arbitrary scaling factors because the value of the RGD is normalized. RGDAC takes values ranging from zero to one. Values near zero represent no consistent correspondence between the two vectors of the RGD, while values near one represent consistent correspondence between the two vectors of the RGD.
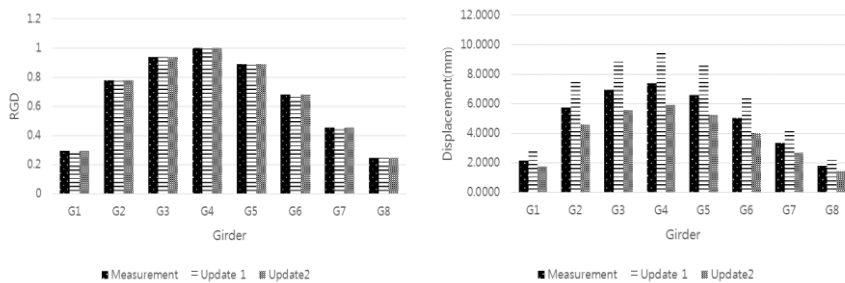
Figure 2. 9 comparison RGD and girder displacement

Table 2. 5 The different displacement in terms of same RGDAC

	True RGD	Updated 1	Updated 2	Updated 3
1st girdier	2.1649	2.8144	1.7319	0.2308
2nd girder	5.7427	7.4655	4.5941	0.6121
3rd girder	6.9453	9.0289	5.5563	0.7403
4th girder	7.3926	9.6104	5.9141	0.788
5th girder	6.5888	8.5654	5.271	1
6th girder	5.0159	6.5207	4.0127	0.8821
7th girder	3.3512	4.3565	2.6809	0.544
8th girder	1.816	2.3608	1.4528	0.2948

2.4 Summary

In this chapter, the procedure of updating the FE model using the dynamic response is presented along with the mathematical issues associated with this procedure. The relative girder displacement (RGD) is used to update the structural variables of the FE model. The RGD can provide the relative stiffness of the structure. However, minimization of the discrepancy between the measured RGD and the RGD from analysis of the FE model may provide a different stiffness distribution because RGD is unlike the static displacement, which is the exact structural response to an applied load. The relative girder displacement assurance criterion (RGDAC) is proposed to ensure a degree of consistency between the measured RGD and the RGD from analysis in the form of a real scalar value. The RGDAC takes values ranging from zero, which represents no consistent correspondence, to one, which represents consistent correspondence between the values from measurement and analysis. The RGD and the RGDAC complement each other by limiting the relative displacement of the girder during the process of updating the FE model.

This research therefore proposes a formulation for the objective function that consists of the residual errors of the natural frequencies, the RGD, and the RGDAC for use in updating the FE model. In addition, each error function is formulated with regard to regularization to produce a single objective function and provide higher weights for the higher residual error solutions. In addition, illustrative examples have been introduced to aid in understanding of the limitations of using either the RGD or the RGDAC alone to update the FE model.

Chapter 3. Numerical Evaluation of the Proposed Method

The model update procedure introduced in this study is examined using numerical examples in this chapter. For the purposes of this examination, the New Jersey Bridge is adopted as the example for study here. The New Jersey Bridge, which is located at Wayne, New Jersey, USA, has a four-span slab and provides two driving lanes in each direction. As a continuously supported bridge with eight plate girders, it represents an appropriate example for the verification of the proposed method. Additionally, a great deal of experimental and analysis data are available for the New Jersey Bridge because it has been the target of extensive investigations. For example, the structural condition of the bridge was evaluated through static and dynamic loading tests as part of the International Bridge Study (IBS) of the Long-Term Bridge Performance (LTBP) Program. This study, which was finalized in 2012 (FHWA, 2012), produced a sophisticated FE analysis model and extensive loading test data, which are both essential factors for the proposed FE model update procedure.

To address the effectiveness of the model update methods, the current status of the target bridge must be known exactly. However, in reality, it is impossible to determine the structural variables of any existing bridge as single values. A simulated bridge model is therefore constructed numerically based on the experimental data that were acquired from the IBS in this study. To formulate the problem, the bending stiffness values of the model will be varied based on some specific assumptions, such as deterioration. For given loading cases, the RGD and the RGDAC for the model update procedure can be acquired from the model. The numerical model would then

be updated to give new optimized variables, which would yield structural responses that are closer to those of the experimental data. The feasibility of the proposed method can be confirmed by investigating the differences between the target and updated values. Because the primary role of the model update procedure is structure condition assessment, the load rating of the bridge must be calculated and investigated thereafter.

3.1 Example using Multi-Girder Bridge Structure

3.1.1 General Description of the New Jersey Bridge

The New Jersey (NJ) Bridge, which was built in 1983, consists of four spans of simply supported composite RC slabs on steel girders. Table 3.1 and Fig. 3.1 show the parts of the bridge structure that were tested along with the definitions of the structural components, where S1 and S2 denote span 1 and span 2, P1 and P2 denote pier 1 and pier 2, A1 and A2 denote abutment 1 and abutment 2, and SB and NB stand for southbound and northbound, respectively, while G1 denotes girder 1. Because only span 2 was freely accessible, most of the tests were performed on span 2. Visual inspections were performed for the bridge components within the accessibility limits. Visual inspection was combined with the application of nondestructive tests (NDTs) for overall evaluation of the bridge condition. Overall estimation of the condition of the bridge structures indicated that the bridge is in good condition. However, some of the bridge components showed deterioration due to environmental action and damage caused by external forces. The NDT equipment used to test the bridge included a Schmidt hammer for concrete strength

measurements, a concrete ultrasonic tester for crack depth measurements, RC radar to detect rebar within the structure, a digital coating thickness gauge for measurement of the paint thickness on the steel girders, and a steel ultrasonic tester to measure the thicknesses of the steel members and detect internal defects within the welded areas. Based on this combination of visual inspection and NDT, the condition of the bridge was assessed at the member level, the span level and finally the bridge level according to Korean Regulations.

The condition of the NJ Bridge was evaluated based on the results of the visual inspection. The calculated damage index was 0.343, which led to a status grade of "C" at bridge level, as shown in Table 3.2. The "C" rating indicates that the bridge has minor problems in a wide range of its primary and/or secondary members and should therefore be repaired to maintain both safety and serviceability performance. Typical weaknesses in these bridges include corrosion of the steel girders and bearings, cracks in the abutments and the bridge structures, and deterioration of the expansion joints. These problematic members make the condition of the bridge legs worse. Corrosion of the steel girders and bearings is concentrated solely on the outer members, but depending on the condition grade at the span level, the worst grade of each member is regarded as the span level grade of that member. Therefore, the span level condition of the girders and the bearings is also assessed at "C". In addition, the expansion joint state was also assessed at "C" to account for leakage.

Table 3. 1 Investigated Structural components (Federal Highway Administration [FHWA], 2012)

Test		Structural components	Purpose of test
Visual inspection / NDT		S1, S2, P1, P2, A1	Condition assessment
Ambient vibration test	Acceleration measurement	SB - S2	Modal analysis finite element model update
	Displacement measurement		Non-contact measurement of displacement Dynamic effect of truck loadings
Local damage monitoring		SB-S2-G1	Local damage detection
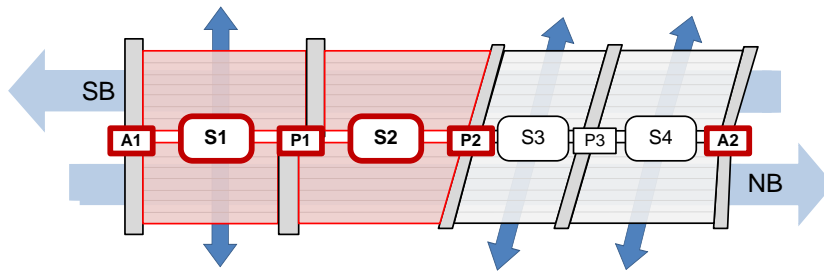
Figure 3. 1 Structural components inspected by Korean Joint Team: span 1, span 2, abutment 1, abutment 2, pier 1, and pier 2 (Federal Highway Administration [FHWA], 2012)

Table 3. 2 Bridge condition rating result (Federal Highway Administration [FHWA], 2012)

Span #	Type	Superstructure			Support #	Substructure	Bearing	Miscellaneous members		
		Slab	Girder	CB		Abut/Pier		Expansion joint	Pavement	Curb
1	SPG	b	c	b	A1	e	c	c	b	b
2	SPG	b	c	b	P1	b	b	c	b	b
3	SPG	b	c	b	P2	b	b	c	b	b
4	SPG	b	c	b	P3	b	b	c	b	b
					A2	e	c	c		
Average (A)		0.2	0.4	0.2	-	0.52	0.28	0.4	0.2	0.2
Weighting factor(W)		23	22	5	-	23	9	9	7	2
(A*W)/ $\sum$ W		0.046	0.088	0.01	-	0.120	0.025	0.036	0.014	0.004

Damage Index	0.343
Condition Rating	C

Field testing of the bridge took place over a period of five days from June 6th to June 10th, 2011. An ambient vibration test (AVT) was performed on southbound span 2 (SB-S2). Two different types of sensors (conventional accelerometers and vision-based systems) were used to measure the vibration of the superstructure caused by the ambient traffic on the bridge. The measured acceleration was applied to assess the soil-structure interaction (SSI) to determine the modal characteristics that represent the overall structural property values, including the inertia, damping, and stiffness information. The dominant natural frequencies and mode shapes that were identified in the AVT showed good agreement with the reported results. The natural frequencies and the mode shapes were then used to perform further updates of the FE model of the bridge. To measure the ambient vibration of the bridge, 16 accelerometers were installed on the lower flange of a single girder, as shown in Fig. 3.2. Fifteen of the accelerometers were placed in the vertical direction while the remaining accelerometer was placed in the lateral direction, as shown in Fig. 3.2. The target for the vision system was attached to the web of girder 1 (G1), and the vision system was then installed on the ground at a distance of approximately 15 m from the target, as shown in Fig. 3.3. The acceleration data were measured simultaneously on channel 2 and using the vision system for comparison purposes.
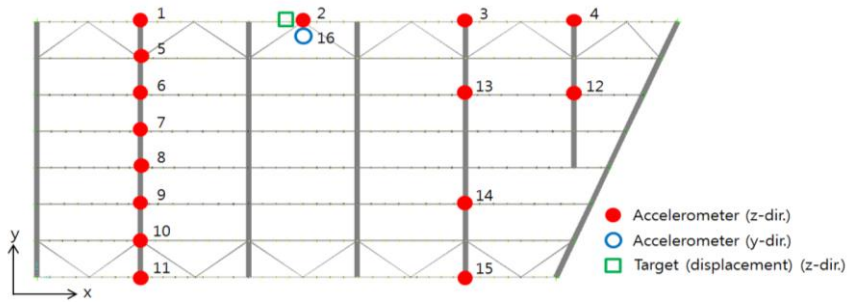
Figure 3. 2 Sensor layout on the bridge (FHWA, 2012)

Figure 3. 3 Target and camcorder used for the displacement (FHWA, 2012)

2.8606 Hz (1.5058)

3.2933 Hz (2.768)

3.7445 Hz (8.9563)

4.5415 Hz (2.7229)

5.3649 Hz (2.4147)

8.1677 Hz (2.4187)

9.3347 Hz (2.4067)

9.4455 Hz (2.2924)

12.009 Hz (2.8544)
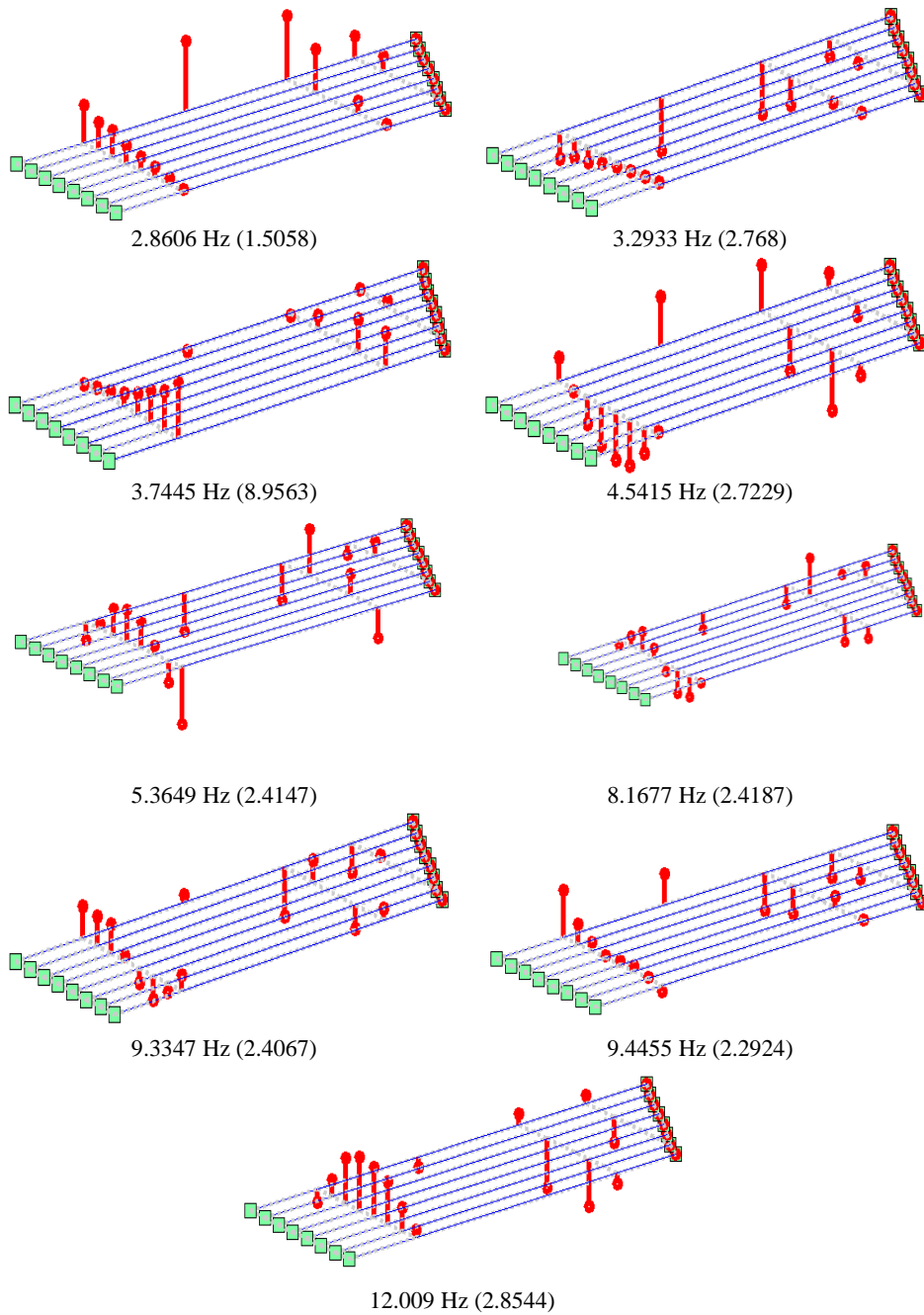
Figure 3. 4 Identified modal properties (where the numbers in parentheses indicate the corresponding damping ratios) (FHWA, 2012)

35

In addition to measuring the modal characteristics of bridges, displacement is also measured by two non-contact methods that reconstruct dynamic displacements from measured accelerations using vision-based methods and finite impulse response filter theory. The dynamic displacements measured by the two non-contact methods agree well with each other. The estimated dynamic amplification factor from the measured displacement is 1.18. The measured displacement also successfully captures the natural frequency of the first mode. The measured modal characteristics are shown in Figure 3.4 and Table 3.3.

Table 3. 3 Summary of identified modal properties (FHWA, 2012)

Mode No.	Frequency (Hz)	Damping ratio	Description
1	2.8606	1.5058	Bending (B1)
-	3.2933	2.768	Unstable/Not used in updating
2	3.7445	8.9563	Torsion(T1)
-	4.5415	2.7229	Unstable/Not used in updating
3	5.3649	2.4147	Lateral (L1)
4	8.1677	2.4187	Lateral (L2)
-	9.3347	2.4067	Unstable/Not used in updating
5	9.4455	2.2924	Torsion(T2)
6	12.009	2.8544	Lateral + Bending (C1)

3.1.2 Sophisticated Finite Element Model of New Jersey Bridge

While the target bridge has a composite cross-section composed of concrete RC slabs and plate girders, the components are modeled independently here for simplification. First, the concrete slab is modeled using eight-node 3D solid elements containing embedded rebar. During placement of the rebar, the weight density is adjusted by considering its contribution to the total mass of the composite cross-section of the

slab. The web and the flanges of the steel girders are modeled using four-node 3D plate elements, known as Kirchhoff plates, with stiffeners. Based on consideration of the small deformation and the low thickness of the member, the use of Kirchoff plate elements is valid. Similarly, the bracing and cross-frames that connect the girder are modeled using a two-node prism 3D beam element called the Timoshenko beam. After field load testing, the FE model is updated through a manual tuning process to produce responses that are closer to the measured data obtained from visual inspection, NDTs, AVTs, and engineering judgment.
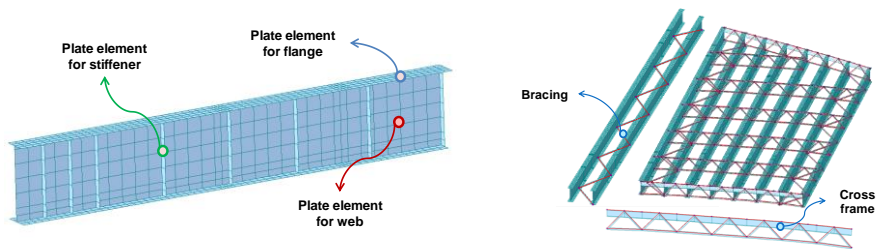
Figure 3. 5 Modeling of the girder and the bracing/cross-frame (FHWA, 2012)

(a) Isometric view

(b) Top view

(c) Front view

(d) Side view
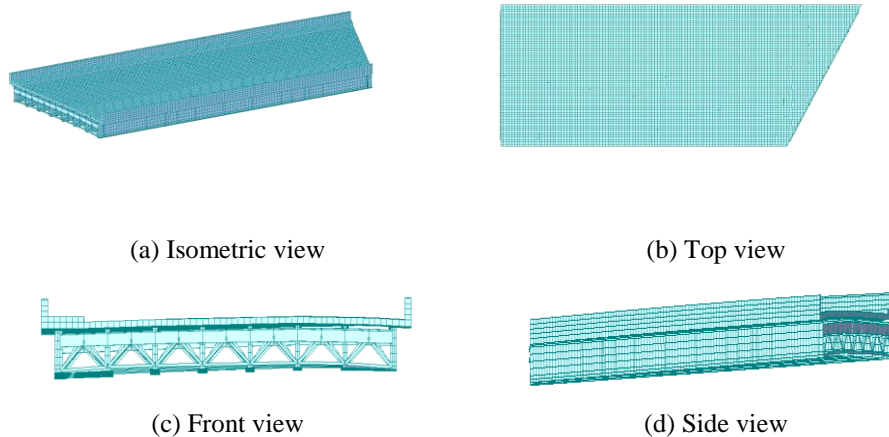
Figure 3. 6 Various views of the constructed model

The natural frequencies that were obtained from the analytical model and from the AVT show a slight discrepancy. Manual tuning of the FE model resulted in an update that produced a unique frequency that was close to the measured value, as shown in Table 3.6.

Table 3. 4 Modal analysis results from the sophisticated FE model
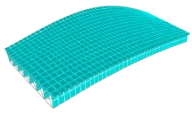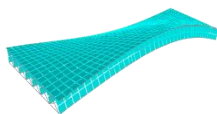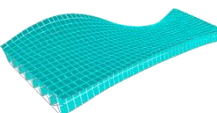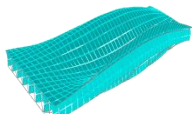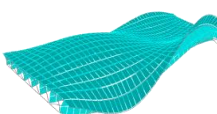
Mode	Frequency (Hz)	Mode shapes	Mode	Frequency (Hz)	Mode shapes
1 (B1)	2.6448		2 (T1)	3.4494	
3 (L1)	6.0060		4 (T2)	7.8064	
5 (L2)	10.1833		6 (C1)	11.8343	

Table 3. 5 Discrepancies between natural frequencies from measurements and analysis

Mode No.	Measured frequency (Hz)	Analyzed frequency (Hz)	Discrepancy (%)	Description
1	2.8606	2.6448	-7.54%	Bending (B1)
2	3.7445	3.4494	-7.88%	Torsion(T1)
3	5.3649	6.006	11.95%	Lateral (L1)
4	8.1677	7.8064	-4.42%	Lateral (L2)
5	9.4455	10.1833	7.81%	Torsion(T2)
6	12.009	11.8343	-1.45%	Lateral + Bending (C1)

3.2 Baseline Finite Element Model and Simulated Bridge Model

3.2.1 Baseline Finite Element Model based on the Sophisticated Finite Element Model

The simulated bridge model based on the NJ Bridge is modeled using the commercial finite element analysis program SAP2000, as shown in Figure 3.7, based on the sophisticated FE model defined in Figs. 3.5 and 3.6. The concrete slab is modeled using shell elements. The steel girders and the cross-beams are modeled using frame elements. Because the shell-frame FE model contains fewer structural parameters than the sophisticated FE model, it has the advantage of reduced computation time requirements when solving the optimization problem and minimizing the differences between the measured data and the analytical values.

Table 3. 6 Material properties used in the shell-frame FE model

		Elastic modulus (Kg/N)	Weight density (Kg/N)
Slab		2.036 E+10	1.271
Steel members	Girder	1.9 E +11	1.271
	Cross-frame	1.599 E +11	4.105 E-1

At this stage, the simplified shell-frame FE model should show the same structural behavior as the actual bridge. The structural parameter values of the shell-frame FE model, which include the material properties shown in Table 3.6 and the sectional properties shown in Table 3.7, come from the sophisticated FE model, and the structural validity of the shell-frame FE model was verified by comparing the structural analysis values of the shell-frame FE model with the corresponding structural analysis values of the sophisticated model. The boundary conditions of the

shell-frame FE model are the spring elements, which are the same as those used for

the sophisticated FE model.
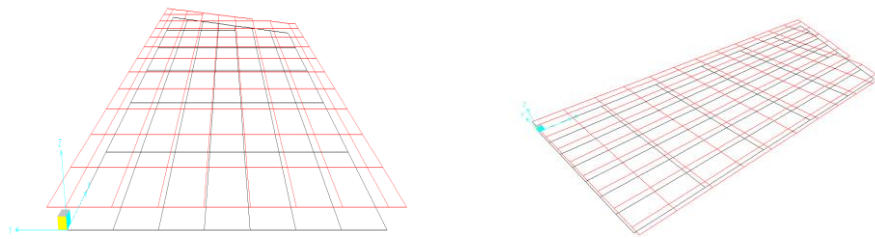
(a) Front view   (b) Isometric view

Figure 3. 7 Frame FE model (in SAP2000)

Table 3. 7 Sectional properties used in the shell-frame FE model

	Area (m^2)	Torsional stiffness (Kg/m^2)	z-direction moment of inertia (m^4)	y-direction moment of inertia (m^4)
1st girder	6.04E-02	3.78E-05	3.36E-02	2.46E-03
2nd girder	6.44E-02	5.83E-05	4.59E-02	1.48E-03
3rd girder	5.46E-02	3.10E-05	2.93E-02	7.81E-04
4th girder	5.46E-02	3.10E-05	2.93E-02	7.81E-04
5th girder	5.05E-02	2.78E-05	2.66E-02	5.62E-04
6th girder	5.05E-02	2.78E-05	2.66E-02	5.62E-04
7th girder	4.53E-02	2.28E-05	2.26E-02	3.77E-04
8th girder	4.53E-02	2.28E-05	2.26E-02	3.77E-04
Cross-frame	7.74E-03	4.16E-06	6.53E-06	2.29E-04

Table 3. 8 Modal analysis results from the baseline frame FE model

Mode	Frequency (Hz)	Mode shapes	Mode	Frequency (Hz)	Mode shapes
1 (B1)	2.5998		2 (T1)	3.1788	
3 (L1)	4.932		4 (T2)	8.2909	
5 (L2)	9.7887		6 (C1)	11.1507	

The structural feasibility of the baseline model is now demonstrated. As shown in Table 3.7, the mode shapes from the shell-frame model are the same as those from the sophisticated FE model. However, there are discrepancies in terms of the natural frequencies of both the sophisticated FE model and the measured data, as shown in Table 3.8 and Table 3.9. In particular, the 1st and 2nd lateral natural frequencies show larger discrepancies when compared with the other natural frequencies. Use of simplified structural members such as slabs, bracing, and cross-frames may provide reduced lateral stiffness when compared with that of the actual bridge. However, the MAC is shown to be nearly one, which indicates that the eigenvectors of the sophisticated and shell-frame models are similar vectors.

A comparison of the natural frequencies of the sophisticated FE model and the shell-frame FE model is shown in Table 3.9, where the discrepancies in the natural frequencies of the bending and torsion mode shapes range from only 1.70% to 7.84%, which indicates that the frame modeling approach is sufficient to represent the primary behavior of the bridge, although the discrepancies in the natural frequencies of the lateral mode shapes show low agreement levels of 17.88% to 24.54%.

Table 3. 9 Discrepancies between natural frequencies of sophisticated and frame FE models

Mode No.	Sophisticated frequency (Hz)	Frame model frequency (Hz)	Discrepancy (%)	Description
1	2.6448	2.5998	1.70%	Bending (B1)
2	3.4494	3.1788	7.84%	Torsion(T1)
3	6.006	4.932	17.88%	Lateral (L1)
4	7.8064	5.8909	24.54%	Lateral (L2)
5	10.1833	9.7887	3.87%	Torsion(T2)
6	11.8343	11.1507	5.78%	Lateral + Bending (C1)

Table 3. 10 Discrepancies between natural frequencies of measured and frame FE models

Mode No.	Measured frequency (Hz)	Frame model frequency (Hz)	Discrepancy (%)	Description
1	2.8606	2.5998	9.12%	Bending (B1)
2	3.7445	3.1788	15.11%	Torsion(T1)
3	5.3649	4.932	8.07%	Lateral (L1)
4	8.1677	5.8909	27.88%	Lateral (L2)
5	9.4455	9.7887	-3.63%	Torsion(T2)
6	12.009	11.1507	7.15%	Lateral + Bending(C1)

A comparison of the natural frequencies from the shell-frame FE model and from the measured data taken from AVT tests is shown in Table 3.10. The discrepancies between the natural frequencies of the bending and torsion mode shapes range from −3.63% to 15.11%, and the discrepancies between the natural frequencies of the lateral mode shapes range from 8.07% to 27.88%.

3.2.2 Virtual Measurement Data from the Simulated Bridge Model

The FE model update procedure using the measured data involves solution of optimization problems to determine the optimal structural parameters (Park et al., 2012). Conventional update procedures typically provide minimized discrepancies between the measurement data and the values from analysis. However, the process of updating the finite element model is an ill-posed inverse problem, which means that the uniqueness of the solution is not guaranteed. Here, simulated bridge models were composed using appropriately assumed flexural stiffness values for the girder to improve the convergence rate of the problem. Then, the optimization problem can be solved using the structural values from analysis, such as the displacement, the natural frequency, and the mode shapes, as virtual measurement data.

Table 3. 11 Flexural stiffness values where one of the inner girders is weaker than the others

	Flexural stiffness($lbf \cdot in^2$)
1st girder	1.544E+12
2nd girder	1.515E+12
3rd girder	1.320E+12
4th girder	1.952E+12
5th girder	1.638E+12
6th girder	1.264E+12
7th girder	1.636 E+12
8th girder	1.728 E+12

Table 3. 12 Flexural stiffness values where some of the inner and outer girders are weaker than the remainder

	Flexural stiffness($lbf \cdot in^2$)
1st girder	2.196E+12
2nd girder	2.596E+12
3rd girder	1.576E+12
4th girder	1.984E+12
5th girder	1.736E+12
6th girder	1.529E+12
7th girder	1.658E+12
8th girder	1.562E+12

Table 3. 13 Flexural stiffness values of the girders when randomly selected using a uniform probabilistic distribution

	Flexural stiffness ($lbf \cdot in^2$)	Flexural stiffness ($lbf \cdot in^2$)	Flexural stiffness ($lbf \cdot in^2$)	Flexural stiffness ($lbf \cdot in^2$)
	$\pm5\%$ variation	$\pm10\%$ variation	$\pm15\%$ variation	$\pm20\%$ variation
1st girder	2.400E+12	2.400E+12	2.225E+12	2.083E+12
2nd girder	3.042E+12	3.193E+12	3.047E+12	3.010E+12
3rd girder	2.079E+12	1.976E+12	1.828E+12	2.158E+12
4th girder	1.997E+12	2.141E+12	1.868E+12	1.674E+12
5th girder	1.849E+12	1.802E+12	1.758E+12	1.564E+12
6th girder	1.846E+12	1.765E+12	2.032E+12	1.902E+12
7th girder	1.630E+12	1.579E+12	1.486E+12	1.551E+12
8th girder	1.526E+12	1.655E+12	1.547E+12	1.699E+12

In this study, the flexural stiffness conditions of multiple girder bridges are divided into three groups to cover general aging and the corresponding changes in

the structural variables of an operational bridge. First, it is assumed that the flexural stiffness of one inner girder is relatively small when compared with the flexural stiffnesses of the other girders. Second, it assumed that the flexural stiffnesses of some of the inner girders and outer girders are similar. Finally, it is assumed that the stiffness of the girder is randomly distributed using a uniform probabilistic distribution. Table 3.11, Table 3.12, and Table 3.13 show the corresponding flexural stiffness values.

3.3 Finite Element Model Updates through an Optimization Procedure

3.3.1 Selection of Optimization Parameters

The data that were measured in the field tests provide a variety of information about the behavior of the actual bridge. Using this information, the updated FE model shows bridge behavior similar to that of the actual bridges, and the bridge performance can be evaluated using structural parameter values with this type of behavior. One important point to remember when updating the finite element model is to consider sufficient numbers of structural parameters to describe the bridge behavior because updating of the finite element model is an optimization problem related to determination of suitable structural parameter values that minimize the mismatch between the measured and analytical structural responses. However, if too many structural parameters are considered, the FE model may then not be optimized properly. Additionally, if too few structural parameters are used, then the proposed FE model may not be able to express the structural behavior of the actual bridge.

Therefore, it is important to perform a sensitivity check as part of the process before updating the FE model.

Four steps are therefore proposed to determine effective structural parameters that are related to the behavior of multiple girder bridges. The first step involves creation of 100 random FE models based on the baseline FE model. The second step is a sensitivity check based on evaluation of the errors of each random model for both the static displacement and the natural frequencies. The discrepancies between the measured and analytical natural frequencies and static displacements are given by Eq. (3.1) and Eq. (3.2), respectively:

$$e(x)_f = \frac{1}{N}\sum_{j=1}^{N}\left(\frac{f(x)_j^a - f_j^m}{f_j^m}\right)^2 \tag{3.1}$$

$$e(x)_\delta = \frac{1}{M}\sum_{i=1}^{M}\left(\frac{\delta(x)_i^a - \delta_i^m}{\delta_i^m}\right)^2 \tag{3.2}$$

where $e(x)_f$ is the residual of natural frequency, f_j is j-th natural frequency(j=1~ number of natural frequency, N=6), $e(x)_\delta$ is the residual of static displacement, δ_i is i-th girder vertical displacement (i=1~number of girder, N=8) and the superscripts a and m represent the analyzed from the finite element model and measured data. The third step is to characterize structural parameters by applying Principal Component Analysis (PCA) to the sensitivity matrix. The analyzed structural variables are shown in Figure 3.8, the length of the vector represents the importance of structural parameter to select structural parameters according to the bridge behavior, and direction of vector represent characteristic of the structural parameter for grouping similar characteristic. The final step is to select key structural

parameters for the bridge behavior and group the structural parameters into similar characteristics.
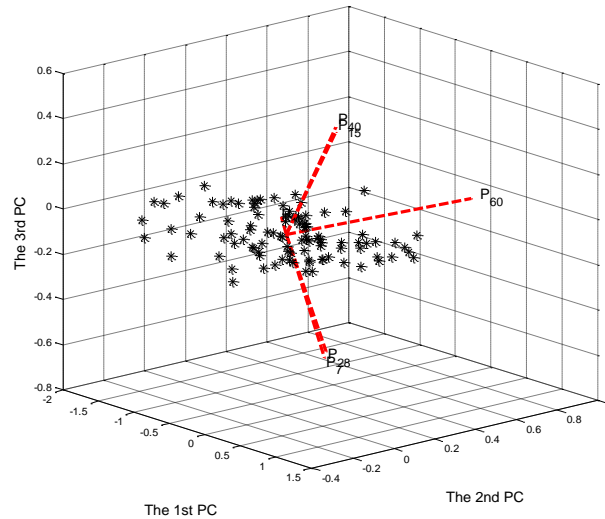
Figure 3. 8 Selection of structural parameters using PCA (Kim, 2015)

A total of 220 structural parameters that can be used to represent the complex behavior of multiple girder bridges is preselected based on considerations of the slabs, girders, and cross-frame of the structure in terms of their mass, elastic modulus, moment of inertia, and torsional stiffness. Finally, using the characteristics of the analyzed structural variables, structural variables with similar sensitivities were grouped together and those with low sensitivity were reduced based on the location of the structural member; 55 structural variables, which are the values of five variables such as mass, elasticity, torsional stiffness, and moment of inertia for 11 different structural members, were then selected as shown in Table 3.14. The optimal structural parameters are then identified by a sequential quadratic programming (SQP) process. As a result, the updated model shows errors of less than 5% for the

summation of the static displacement and for the natural frequencies of both the measured data and the analytical values.

Table 3. 14 Selected structural variables and variation used for optimization

	Variables	No. of members	Variation for optimization
m	Mass	Girder – 8ea Cross frame – 1ea Frame at support – 1ea Slab shell – 1ea	$-20\% \leq$ initial value $\leq +20\%$
E	Young's modulus		$-30\% \leq$ initial value $\leq +30\%$
J	Torsional stiffness		$-15\% \leq$ initial value $\leq +15\%$
I_{yy}	Moment of inertia		$-15\% \leq$ initial value $\leq +15\%$
I_{zz}	Moment of inertia		$-15\% \leq$ initial value $\leq +15\%$

3.3.2 Optimization Algorithm

The problem of updating the finite element model can be expressed as a constrained nonlinear multivariate optimization problem based on consideration of the error function of the objective function and constraints. Optimization for system identification using limited experimental measurements usually leads to an ill-posed problem in which the number of measurement data is less than the number of optimization variables. In addition, numerous different uncertainties have been indicated, including uncertainties in the measurement data and the FE modeling process. Extensive research has been conducted over the last few decades to overcome these limitations and find suitable structural parameters for the FE model that produce the same structural behavior from both the measurement data and the FE model. Among the proposed approaches, use of a genetic algorithm (GA) is regarded as a new way to solve nonlinear programming problems that was developed

by Duffin, Peterson, and Zener. In this research, the optimization process required to minimize the discrepancies between the measurement data and the values from analysis uses an iterative method based on a GA, which is categorized as a global solution.

Determination of the convergence condition when using the GA technique is as important as explicit construction of the objective function. The convergence criteria for the GA vary when the value of the objective function satisfies the convergence criteria until the objective function value does not change for a certain generation, which is called stall generation, or until the maximum number of generations is reached. To confirm the convergence of the GA, the convergence process was analyzed through consideration of the 10 cases shown in Table 3.15.

Table 3. 15 Ten cases used for analysis of the convergence criteria

	Consideration
Population	88, 150, 200, 300
Generation	200, 300, 500
Stall Generation	50, 100, 200

Analysis of the convergence process showed that all the numerical examples existed in the 200th generation, and even if the objective function value was changed for the 50th generation, the 100th generation, and the 200th generation, there was no significant effect on the optimization results. Additionally, when the population number is 300, the optimization results are better than when the population number is 200, but when the population is 500, there are no significant differences in the results. Consequently, in this study, the convergence criteria are defined as 200

generations in which each generation has a population of 300 and 50 generations during which the objective function value does not change continuously.
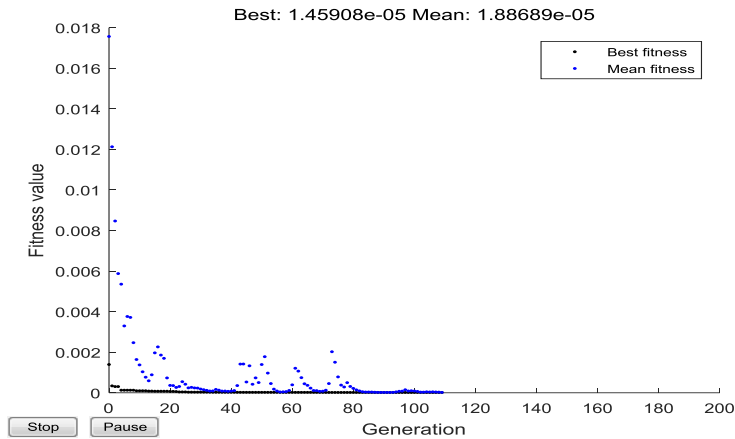
Figure 3. 9 Fitness value curve in the GA procedure

3.4 Comparison of Update Performances of Various Objective Functions

The proposed method is validated by constructing a simulated bridge model, and the effectiveness of the method is defined by comparison with the existing method used to construct the objective function. The flexural stiffness of the girders is defined as shown in Table 3.11, where the flexural stiffness of one of the inner girders is weaker than all the others.

3.4.1 Description of Virtual Measurement Data

As shown in Fig. 3.10, when the analytical values of the simulated bridge model are assumed to be the virtual measurement data, the vertical displacements at the

midpoint of each girder and the natural frequencies ranging up to the sixth order that were generated using the second-lane load are then used to update the baseline FE model. The load magnitude was that of the lane load (MLTM, 2012) given in the Korean Bridge Design Specification.
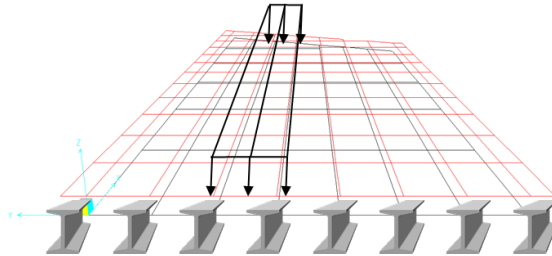
Figure 3. 10 Location of the lane load in the FE model

The discrepancies between the natural frequencies of the virtual measurement data and those of the baseline model that is to be used for optimization are shown in Table 3.16. The discrepancies in the vertical displacements of each girder are shown in Fig. 3.11.

Table 3. 16 Discrepancy of natural frequencies between simulated and baseline

Mode No.	Measured frequency (Hz)	Baseline frequency (Hz)	Discrepancy (%)	Description
1	2.471	2.6448	-7.03%	Bending (B1)
2	3.069	3.4494	-12.39%	Torsion(T1)
3	4.829	6.006	-24.37%	Lateral (L1)
4	8.157	7.8064	4.30%	Lateral (L2)
5	9.398	10.1833	-8.36%	Torsion(T2)
6	10.538	11.8343	-12.30%	Lateral + Bending(C1)
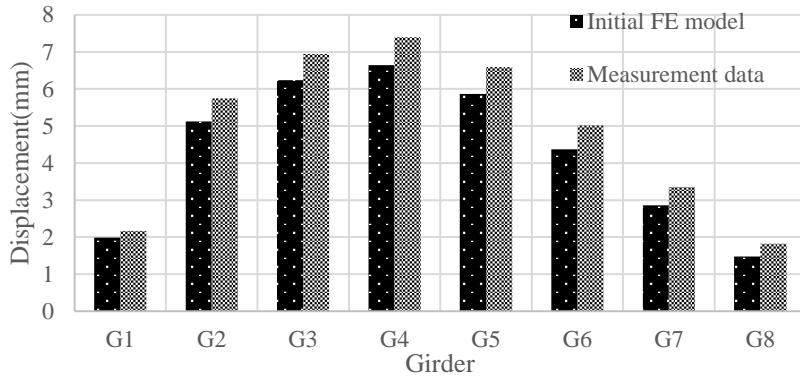
Figure 3. 11 Discrepancies between natural frequencies of simulated data and baseline model

3.4.2 Formulation of Objective Functions

As shown in Table 3.17, five different objective functions for the optimization process are constructed differently to verify the proposed method and for comparison with the previous method. The objective function used for the first case consists of the errors of the natural frequencies and the RGD, while the objective function for the second case consists of the errors of the natural frequencies and the RGDAC; the objective function for the third case consists of the errors of the natural frequencies, the RGD and the RGDAC. The objective function for the fourth case consists of the natural frequencies and the MAC in the case where the bridge traffic could not be controlled and the FE model is updated using dynamic measurement data only. Finally, the objective function for the fifth case consists of the natural frequency, the MAC, and the static displacement in the case where the FE model is updated using both the static and dynamic measurement data obtained through traffic control procedures on the bridge.

The objective function used to update the baseline FE model is composed of error functions, which are defined in chapter 2.2. The objective function that

51

describes the discrepancy between the measured and analytical natural frequencies and RGD values is given as Eq. (3.3):

$$min\,J1(x) = \frac{1}{N}\sum_{j=1}^{N}\left(\frac{f(x)_j^a - f_j^m}{f_j^m}\right)^2 + \frac{1}{M}\sum_{i=1}^{M}\left(\frac{RGD(x)_i^a - RGD_i^m}{RGD_i^m}\right)^2 \qquad (3.3)$$

The objective function that describes the discrepancy between the measured and analytical natural frequencies and the RGDAC values is given as shown in Eq. (3.4):

$$min\,J2(x) = \frac{1}{N}\sum_{j=1}^{N}\left(\frac{f(x)_j^a - f_j^m}{f_j^m}\right)^2 + \frac{(1-\sqrt{RGDAC})^2}{RGDAC} \qquad (3.4)$$

The objective function that describes the discrepancy between the measured and analytical natural frequencies, the RGD values, and the RGDAC values is given as Eq. (3.5):

$$min\,J3(x) = \frac{1}{N}\sum_{j=1}^{N}\left(\frac{f(x)_j^a - f_j^m}{f_j^m}\right)^2 + \frac{1}{M}\sum_{i=1}^{M}\left(\frac{RGD(x)_i^a - RGD_i^m}{RGD_i^m}\right)^2 + \frac{(1-\sqrt{RGDAC})^2}{RGDAC} \qquad (3.5)$$

The objective function that describes the discrepancy between the measured and analytical natural frequencies and the MAC values is given as Eq. (3.6):

$$min\,J4(x) = \frac{1}{N}\sum_{j=1}^{N}\left(\frac{f(x)_j^a - f_j^m}{f_j^m}\right)^2 + \frac{1}{N}\sum_{j=1}^{N}\frac{(1-\sqrt{MAC_j})^2}{MAC_j} \qquad (3.6)$$

The objective function that describes the discrepancy between the measured and analytical natural frequencies and the static displacement values is given as Eq. (3.7):

$$min\,J5(x) = \frac{1}{N}\sum_{j=1}^{N}\left(\frac{f(x)_j^a - f_j^m}{f_j^m}\right)^2 + \frac{1}{M}\sum_{i=1}^{M}\left(\frac{\delta(x)_i^a - \delta_i^m}{\delta_i^m}\right)^2 \qquad (3.7)$$

Table 3. 17 Objective functions used for case study

	e_{NF}	e_{MAC}	e_{DISP}	e_{RGD}	e_{RGDAC}	Objective Function
Case 1	●			●		$\min J1(x) = \min(e_{NF} + e_{RGD})$
Case 2	●				●	$\min J2(x) = \min(e_{NF} + e_{RGDAC})$
Case 3	●			●	●	$\min J3(x) = \min(e_{NF} + e_{RGD} + e_{RGDAC})$
Case 4	●	●				$\min J4(x) = \min(e_{NF} + e_{MAC})$
Case 5	●	●	●			$\min J5(x) = \min(e_{NF} + e_{MAC} + e_{DISP})$

3.4.3 Comparison of Structural Responses

For comparison of cases 1 to 3, in which the baseline FE model is updated using the RGD, the analytical values of the updated FE model and the measurement data are compared. As shown in Table 3.18, the discrepancies between the natural frequencies of the measurement data and those of the updated FE model are similar, as shown in Fig. 3.12.

Table 3. 18 Natural frequencies from the measured data and the updated FE model

Mode No.	Frequency (Hz)			
	Measured	Case 1	Case 2	Case 3
1 (B1)	2.471	2.462	2.471	2.468
2 (T1)	3.069	3.072	3.070	3.069
3 (L1)	4.829	4.826	4.833	4.829
4 (L2)	8.157	8.159	8.155	8.157
5 (T2)	9.398	9.428	9.385	9.407
6 C1)	10.538	10.541	10.528	10.544
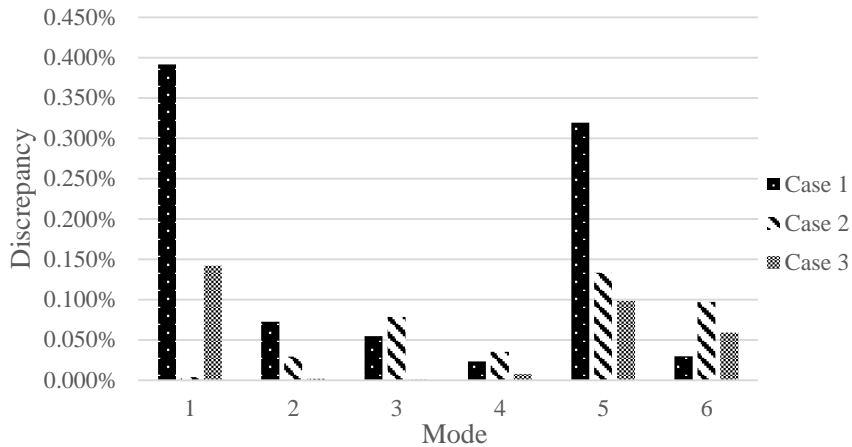
Figure 3. 12 Discrepancies between the natural frequencies of the measured data and the updated model cases

The cases where only the RGD (case 1) or the RGDAC (case 2) are used and the case where both the RGD and the RGDAC (case 3) are used are compared in terms of the results of updating the baseline FE model. The method used to construct each objective function has a similar updating effect on the model. However, a comparison of the updated results for the static displacement is shown in Figure 3.13, and the case where both the RGD and the RGDAC are used (case 3) provides the best updated results, while the case where only the RGDAC is used (case 2) provides the worst updated results.
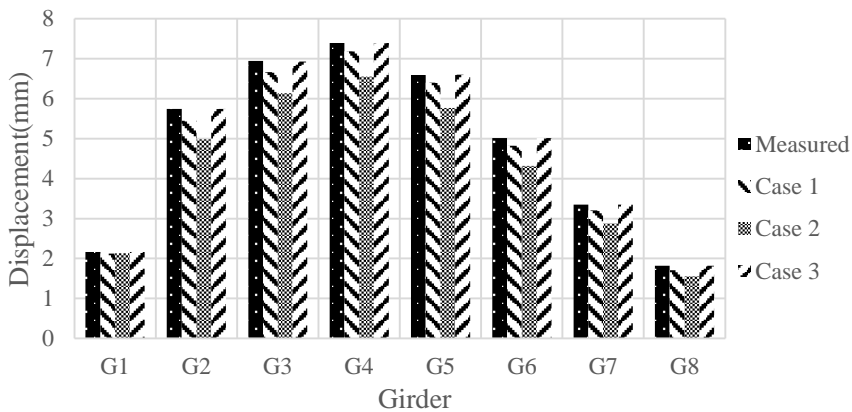
Figure 3. 13 Discrepancies between static displacement results from measured data and the updated model cases

54

When the FE model is updated using the RGD, the updated results for the natural frequency or the mode shape obtained using the RGD, the RGDAC, or both the RGD and the RGDAC provide the updated results that are closest to the measured value. The results of this case study show that use of the RGD to update the structural parameters provides the measured displacement at each girder while reducing the differences in relative displacement of the girder, but there are still some discrepancies with the measured displacement because the RGD represents a relative ratio, unlike the static displacement. If the entire girder shape is used, as in the RGDAC, the shape of the whole girder can remain the same, but the actual displacement may differ because the RGDAC can only indicate consistency rather than provide validation. Even when the RGDAC value is unity, the RGD and the displacement could represent different arbitrary scales because the value of the RGD is the ratio of displacement with respect to the girder. However, when the objective function consists of both the RGD and the RGDAC (case 3), this provides the smallest displacement discrepancy. Therefore, the RGD and the RGDAC supplement each other in limiting the relative displacement of the girder during the process of updating the finite element model.

For comparison of cases 3 to 5, when the baseline FE model is updated using the proposed method (case3), the analytical values of the updated FE model are compared with the measurement data. Table 3.19 lists the discrepancies between the natural frequencies of the measurement data and those of the updated finite model, and these discrepancies are illustrated in Figure 3.14.

Table 3. 19 Natural frequencies of the measured data and the updated FE model cases

Mode No.	Measured frequency (Hz)	Case 3 frequency (Hz)	Case 4 frequency (Hz)	Case 5 frequency (Hz)
1 (B1)	2.471	2.468	2.471	2.475
2 (T1)	3.069	3.069	3.069	3.082
3 (L1)	4.829	4.829	4.829	4.826
4 (L2)	8.157	8.157	8.158	8.161
5 (T2)	9.398	9.407	9.398	9.361
6 C1)	10.538	10.544	10.538	10.516
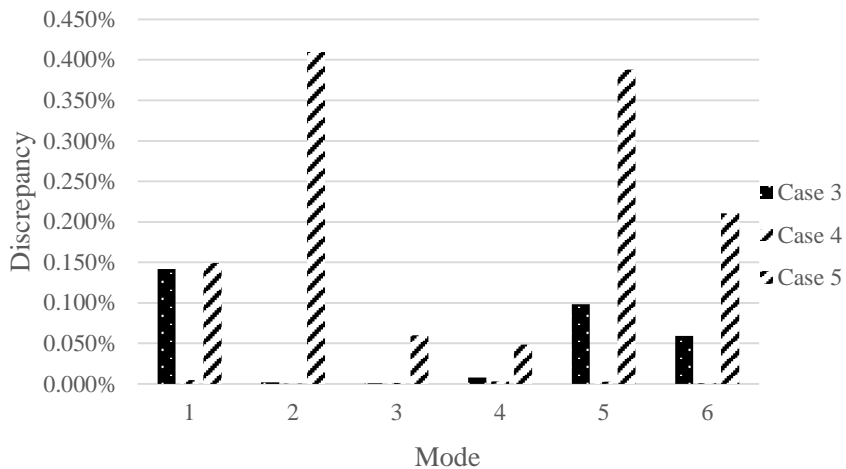
Figure 3. 14 Discrepancies between the natural frequencies of the measured data and the updated model cases

The objective function in the third case consists of the errors in the natural frequencies, and the RGD and the RGDAC provide similar updated results for the natural frequencies and mode shapes. Additionally, as shown in Fig. 3.15, the discrepancy in the static displacement produces the worst update results when the objective function consists of the error function for the dynamic measurement data. The best update results occur when the objective function consists of the error functions of the static and dynamic measurement data and the proposed method provides similar update results.

The case study confirmed that updating of the baseline FE model using all the static and dynamic measurement data produces the results that are the closest to the bridge measurement data. The study also confirmed that the differences in the natural frequencies and the mode shapes could be updated using only the dynamic measurement data, but the difference in the vertical displacement is minimized to a lesser degree than that produced when the objective function consists of both the static and dynamic measurement data. However, if the relative displacement of the girder is used rather than the static displacement through application of the proposed method, it is confirmed that the limitation of use of dynamic measurement data only could be overcome using the relative displacement of the girder rather than the static displacement.
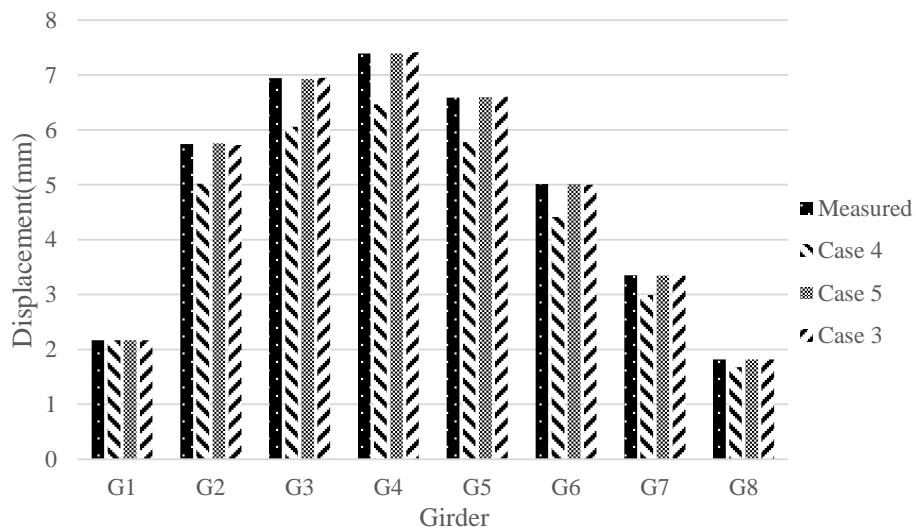
Figure 3. 15 Discrepancies between static displacements of measured and updated model cases

3.4.4 Evaluation of Load Rating

The load and resistance factor rating (LRFR) supports three limit states that follow the load and resistance factor design (LRFD) method. The service limit state, the fatigue limit state, and the strength limit state can be used to evaluate the load rating factor. In addition, the LRFR considers not only the designed load but also the permitted load to check the safety of the bridge using the average daily truck traffic (ADTT). The general LRFR rating is given by Eq. (3.8):

$$\text{RF} = \frac{C - \gamma_{DC}DC - \gamma_{DW}DW \pm \gamma_p P}{\gamma_L LL(1+IM)} \tag{3.8}$$

where C is the structural capacity, DC is the dead-load effect of the structural components, DW is the dead-load effect of the wearing surfaces and utilities, P is permanent loading other than the dead loads, IM is the dynamic load allowance, and LL is the live-load effect. The load factor γ_{DC} is applied to the weight of the structural components, the load factor γ_{DW} is applied to the wearing surfaces and utilities, the load factor γ_p is applied to permanent loads other than the dead loads, and the load factor γ_L is applied to the live-load. These load factors follow the guidelines of the Manual for Bridge Evaluation (2008, American Association of State Highway and Transportation Officials (AASHTO)), as shown in Table 3.20.

Table 3. 20 Load factors used for evaluation of the load rating

γ_{DC}	γ_{DW}	γ_p	IM
1.25	1.50	1.75	0.174

Table 3. 21 Evaluated load ratings and locations

	Case 1	Case 2	Case 3	Case 4	Case 5
Load rating	1.798	1.564	1.857	1.824	1.983
Location	Girder3	Girder 6	Girder 6	Girder 4	Girder 6

As shown in Table 3.21, the evaluated load ratings produced by the proposed method (case 3) show similar results to those in case 5 in terms of both value and location. When the objective function consists of the RGD (case 1) or the RGDAC (case 2) with the natural frequencies, the RGDAC provides the same girder location as both case 5 and case 3 for evaluation of the load rating but gives a lower load rating value. In contrast, the RGD produces a similar load rating value to those of case 5 and case 3, but provides a different girder location for evaluation of the load rating.

3.5 Update Performance of the Proposed Method for Various Lane Loading Cases

The RGD can provide different mathematical values that depend on the ratio criteria defined in chapter 2.1.2 and can also vary depending on where the load is positioned. In this section, to establish the generality of the proposed method, the loading position of the load is varied from the first lane to the fourth lane in the simulated bridge model when the flexural stiffness values of several of the inner and outer girders are similar, and the analytical measurement values are assumed to be virtual measurement data.

3.5.1 Description of Virtual measurement data
As shown in Fig. 3.16, when the analytical values obtained from the simulated bridge model are used as the virtual measurement data, the vertical displacements at the midpoint of each girder and the natural frequencies ranging up to the sixth order

generated by the model from the first lane load to the fourth lane load are used to update the baseline FE model. The load magnitude was that of the lane load (MLTM, 2012), which is used in the Korean Bridge Design Specification.
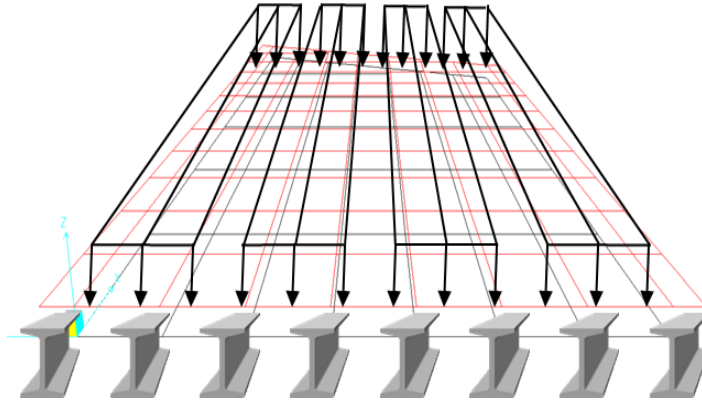
Figure 3. 16 Location of the lane load on the FE model

The discrepancies between the natural frequencies from the virtual measurement data and from the baseline model to be used for optimization range from 1.72 to 21.78%, as shown in Table 3.22. The vertical displacement of each girder is shown in Fig. 3.17, and ranges from the first lane to the fourth lane. Figure 3.18 presents the different RGDs with respect to the applied lane load locations.

Table 3. 22 Discrepancy of natural frequencies between Measured and baseline

Mode No.	Measured frequency (Hz)	Baseline frequency (Hz)	Discrepancy (%)	Description
1	2.4904	2.6448	1.72%	Bending (B1)
2	3.0882	3.4494	8.51%	Torsion (T1)
3	4.8505	6.006	21.78%	Lateral (L1)
4	8.1607	7.8064	-5.84%	Lateral (L2)
5	9.4455	10.1833	4.03%	Torsion (T2)
6	10.6580	11.8343	6.13%	Lateral + Bending(C1)
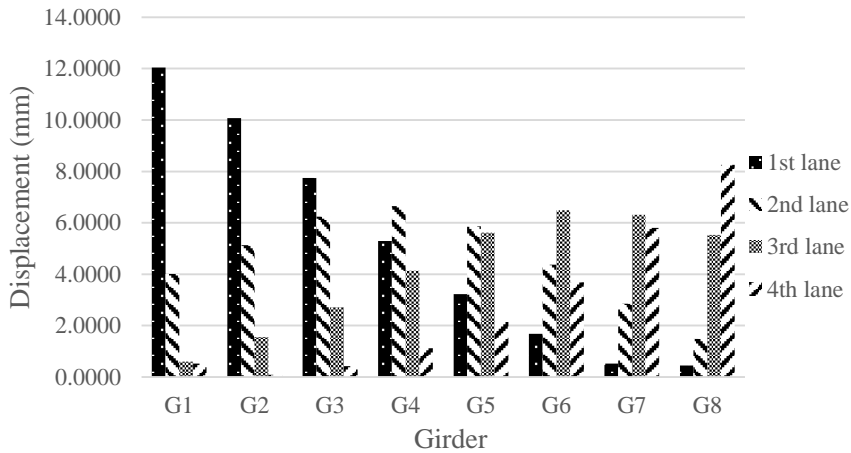
Figure 3. 17 Vertical displacement ranging from the 1st lane to the 4th lane load
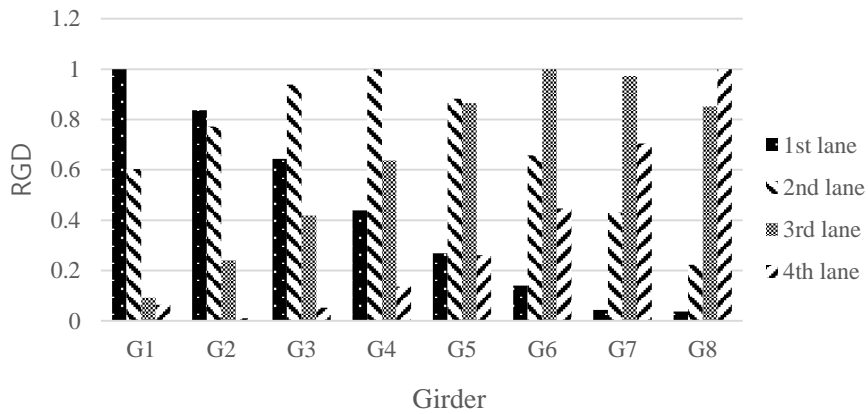
Figure 3. 18 RGD ranging from the 1st lane to the 4th lane load

3.5.2 Formulation of Objective Functions

As shown in Table 3.23, the six different objective functions used for optimization are constructed differently for the generality of the proposed method. The objective function for the first case consists of the error for the natural frequencies when using both the RGD and the RGDAC from the first lane load. The objective function for the second case consists of the error for the natural frequencies when using both the RGD and the RGDAC from the second lane load. The objective

function for the third case consists of the error for the natural frequencies when using both the RGD and the RGDAC from the third lane load. The objective function for the fourth case consists of the error for the natural frequencies when using both the RGD and the RGDAC from the first to fourth lane load. The objective function for the fifth case consists of the natural frequencies and the MAC under the conditions that the bridge traffic could not be controlled and the FE model is updated using dynamic measurement data only. Finally, the objective function for the sixth case consists of the natural frequency, the MAC, and the static displacement under the condition that the FE model is updated using both the static and dynamic measurement data that were obtained through traffic control procedures on the bridge.

Table 3. 23 Objective functions for the case studies

	e_{NF}	e_{MAC}	e_{DISP}	e_{RGD} e_{RGDAC}	Objective Function
Case 1	●		●	●	$\min J1(x) = \min(\, e_{NF} + e_{RGD}^{1st} + e_{RGDAC}^{1st}\,)$
Case 2	●		●	●	$\min J2(x) = \min(\, e_{NF} + e_{RGD}^{2nd} + e_{RGDAC}^{2nd}\,)$
Case 3	●		●	●	$\min J3(x) = \min(\, e_{NF} + e_{RGD}^{3rd} + e_{RGDAC}^{3rd}\,)$
Case 4	●		●	●	$\min J4(x) = \min(\, e_{NF} + e_{RGD}^{4th} + e_{RGDAC}^{4th}\,)$
Case 5	●	●			$\min J5(x) = \min(e_{NF} + e_{MAC})$
Case 6	●	●	●		$\min J6(x) = \min(\, e_{NF} + e_{MAC} + e_{DISP}\,)$

An objective function to update the baseline finite element model is comprised of error functions, which are defined chapter 2.2. The objective function for the discrepancy between measured and analyzed natural frequencies, RGD and RGDAC are equated as Eq. (3.9). Every case has the same objective function, but use different RGD and RGDAC regarding location of lane load.

$$\min J1\sim4(x) = \frac{1}{N}\sum_{j=1}^{N}\left(\frac{f(x)_j^a - f_j^m}{f_j^m}\right)^2 + \frac{1}{M}\sum_{i=1}^{M}\left(\frac{RGD(x)_i^a - RGD_i^m}{RGD_i^m}\right)^2 + \frac{\left(1-\sqrt{RGDAC}\right)^2}{RGDAC}(3.9)$$

The objective function used to determine the discrepancies between the measured and analytical natural frequencies and the MAC values is given as Eq. (3.10):

$$\min J5(x) = \frac{1}{N}\sum_{j=1}^{N}\left(\frac{f(x)_j^a - f_j^m}{f_j^m}\right)^2 + \frac{1}{N}\sum_{j=1}^{N}\frac{\left(1-\sqrt{MAC_j}\right)^2}{MAC_j} \qquad (3.10)$$

The objective function used to determine the discrepancies between the measured and analytical natural frequencies and the static displacement values is given as Eq. (3.11)

$$\min J6(x) = \frac{1}{N}\sum_{j=1}^{N}\left(\frac{f(x)_j^a - f_j^m}{f_j^m}\right)^2 + \frac{1}{M}\sum_{i=1}^{M}\left(\frac{\delta(x)_i^a - \delta_i^m}{\delta_i^m}\right)^2 \qquad (3.11)$$

3.5.3 Comparison of Structural Responses

For comparison of cases 1 to 3, in which the baseline FE model is updated using the relative displacement of the girder, the analytical values of the updated FE model and the measurement data are compared. Table 3.18 shows that the discrepancies

between the natural frequencies of the measurement data and the updated FE model in cases 1 to 3 have similar values, which is also illustrated in Fig. 3.19.

The method used to construct each objective function has a similar updating effect. Even when the RGD and the RGDAC from the fourth lane load location provide relatively higher discrepancies in the natural frequency, comparison of the updated results for the static displacement shown in Figure 3.20 indicates that the updated results provide similar static displacements to those of the measured data.

Table 3. 24 Natural frequencies from the measured data and the updated FE model

Mode No.	Measured frequency (Hz)	Case 1 frequency (Hz)	Case 2 frequency (Hz)	Case 3 frequency (Hz)	Case 4 frequency (Hz)
1 (B1)	2.490	2.490	2.489	2.489	2.509
2 (T1)	3.088	3.089	3.090	3.090	3.093
3 (L1)	4.851	4.850	4.855	4.866	4.885
4 (L2)	8.161	8.204	8.205	8.194	8.188
5 (T2)	9.445	9.462	9.452	9.444	9.527
6 C1)	10.658	10.668	10.665	10.653	10.684
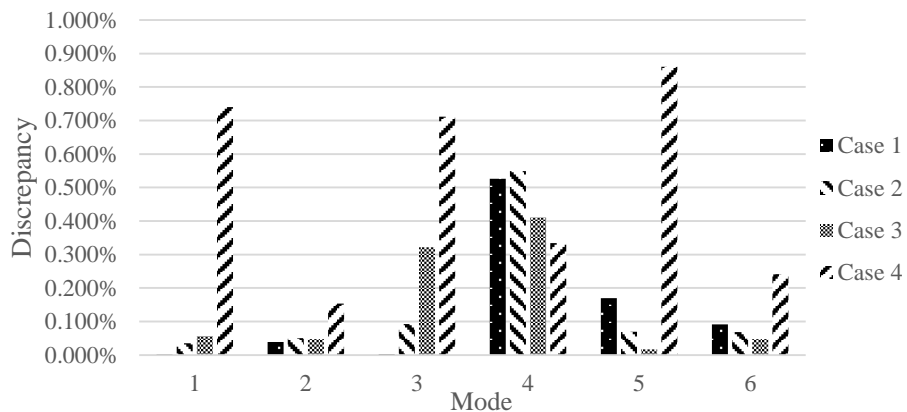
Figure 3. 19 Discrepancies between the natural frequencies of the measured and updated model cases

Figure 3. 20 Discrepancies between the static displacement values of the measured and updated model cases

In the case of the multi-girder bridges used to verify the effectiveness of the proposed method, the updated results for cases 2, 5 and 6 were compared when the flexural stiffness values of several inner girders and outer girders were relatively low when compared with the other girders. When the FE model is updated using the relative displacement of the girder, it provides updated results that are closest to the measured values and provides similar results to those obtained using the static displacement.

Table 3.25 lists the discrepancies between the natural frequencies of the measurement data and those of the updated FE model, which are illustrated in Figure 3.21.

Table 3. 25 Natural frequencies of the measured data and the updated FE model

Mode No.	Measured frequency (Hz)	Case 2 frequency (Hz)	Case 5 frequency (Hz)	Case 6 frequency (Hz)
1 (B1)	2.490	2.489	2.489	2.490
2 (T1)	3.088	3.090	3.090	3.089
3 (L1)	4.851	4.855	4.866	4.846
4 (L2)	8.161	8.205	8.194	8.162
5 (T2)	9.445	9.452	9.444	9.442
6 C1)	10.658	10.665	10.653	10.649
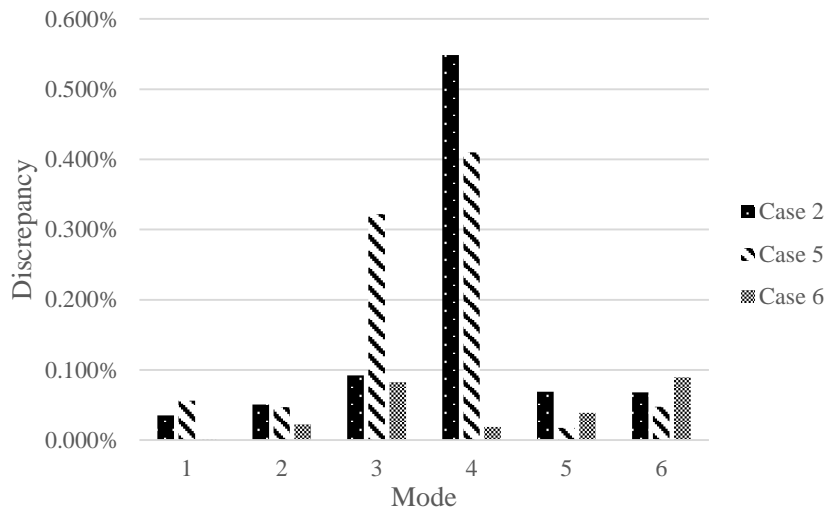
Figure 3. 21 Discrepancies between the natural frequencies of the measured data and the updated model cases

When the flexural stiffness values of several inner girders and outer girders are relatively low in comparison to the values of the other girders, the proposed method (case 2), the method using dynamic data (case 5), and the method using both static and dynamic data (case 6) provide larger discrepancies in terms of lateral mode shape and their natural frequencies. The reason for this update result is that it is difficult to update the FE model for the lateral behavior of the frame FE model when the stiffness values of several of the inner girders and outer girders are similar. It

constantly shows an updated result similar to that shown in chapter 3.4, in which the flexural stiffness of one of the inner girders has the weakest value.

However, as shown in Fig. 3.22, the discrepancies in the static displacement produce the worst update results when the objective function consists of the error function of the dynamic measurement data (case 5). The best update results are produced when the objective function consists of the error functions of the static and dynamic measurement data (case 6) and the proposed method provides similar update results (case 6).
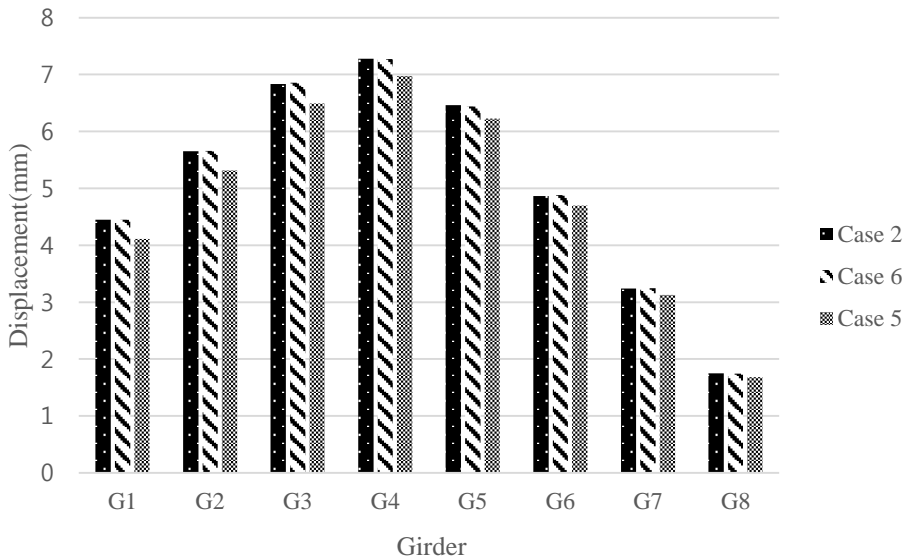
Figure 3. 22 Discrepancies between the static displacements of the measured data and the updated model cases

This case study has shown that when the flexural stiffness values of several inner girders and outer girders have been updated such that they are lower than the other girders, all the static and dynamic measurement data are required to update the

baseline FE model to yield the closest possible result to the bridge measurement data. It is also possible to update discrepancies in the natural frequencies and mode shapes using only the dynamic measurement data, but it is found that the minimum difference in the vertical displacement is less than that when the objective function is configured using both static and dynamic error functions. However, when the relative displacement of the girder is used rather than the static displacement in the proposed method, it was found that the limitations of using only dynamic measurement data can be overcome.

3.5.4 Evaluation of Load Rating

The LRFR supports three limit states that follow the LRFD method. The service limit state, the fatigue limit state and the strength limit state can therefore be evaluated as rating factors. In addition, the LRFR considers not only the designed load but also the permitted load to verify the safety of the bridge using the ADTT. The general LRFR rating is thus given by Eq. (3.12):

$$\text{RF} = \frac{C - \gamma_{DC}DC - \gamma_{DW}DW \pm \gamma_p P}{\gamma_L LL(1+IM)} \tag{3.12}$$

where C is the structural capacity, DC is the dead-load effect of the structural components, DW is the dead-load effect of the wearing surfaces and utilities, P is the permanent loading other than that of the dead loads, IM is the dynamic load allowance and LL is the live-load effect. The load factor γ_{DC} is applied to the weight of the structural components, the load factor γ_{DW} is applied to the wearing surfaces and utilities, the load factor γ_p is applied to permanent loads other than the dead

loads, and the load factor γ_L is applied to the live-load. These load factors again

follow

Table 3. 26 Load factors used for evaluation of the load rating

γ_{DC}	γ_{DW}	γ_p	IM
1.25	1.50	1.75	0.174

Table 3. 27 Evaluated load ratings and locations

	Case 1	Case 2	Case 3	Case 4	Case 5	Case 6
Load rating	1.891	1.748	1.733	1.525	1.937	1.783
Location	Girder 6	Girder 6	Girder 6	Girder 6	Girder 1	Girder 6

As shown in Table 3.21, the load ratings evaluated by the proposed method

(cases 1 to 4) show similar results to those of case 6 in terms of value and location,

except when the RGD and the RGDAC come from the applied fourth lane load (case

4). When the objective function consists of the RGD and the RGDAC with the

natural frequencies, it provides the same girder location as that of case 6 for

evaluation of the load rating and shows a similar load rating value. In contrast, an

objective function consisting of the natural frequencies and the mode shapes shows

a higher load rating value when compared with those of cases 1 to 4 and case 6 and

also provides a different girder location for evaluation of the load rating.

3.6 Updating the Performance of the Proposed Method for Various Cases of the Girder Stiffness Distribution

The RGD could provide different mathematical values that depend on the ratio criteria, as defined in Chapter 2.1.2, when the flexural stiffness of the girder is randomly defined. In this chapter, the flexural stiffness of the girder is defined using the uniform probabilistic distribution from the baseline, and a total of four cases are considered within variation ranges of $\pm5\%, \pm10\%, \pm15\%, \pm20\%$ to establish the generality of the proposed method, while the analytical measurement values are assumed to be virtual measurement data.

3.6.1 Description of the Virtual measurement data

As shown in Figure 3.23, when the analytical values of the simulated bridge model are assumed to be virtual measurement data, the vertical displacement at the midpoint of each girder and the natural frequencies ranging up to the sixth order that are generated by application of the second lane load are used to update the baseline FE model. The load magnitude was again the lane load (MLTM, 2012), which is used in the Korean Bridge Design Specification.
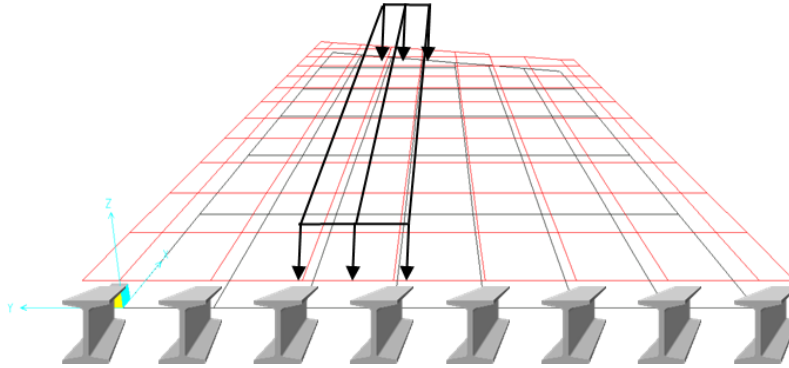
Figure 3. 23 Location of the lane load in the finite element model

The girder flexural stiffness is defined using the uniform probabilistic distribution from the baseline model, and a total of four cases are considered within variation ranges of $5\%, \pm 10\%, \pm 15\%, \pm 20\%$ to establish the generality of the proposed method, where the analytical measurement values are assumed to be virtual measurement data. Table 3.28 shows the simulated flexural stiffness values in terms of their variations and Fig. 3.24 shows the probabilistic distributed elasticity and the base elasticity of the girder.

Table 3. 28 Simulated flexural stiffness values in terms of their variation

	±5%	±10%	±15%	±20%
G1	2.40E+12	2.40E+12	2.23E+12	2.08E+12
G2	3.04E+12	3.19E+12	3.05E+12	3.01E+12
G3	2.08E+12	1.98E+12	1.83E+12	2.16E+12
G4	2.00E+12	2.14E+12	1.87E+12	1.67E+12
G5	1.85E+12	1.80E+12	1.76E+12	1.56E+12
G6	1.85E+12	1.77E+12	2.03E+12	1.90E+12
G7	1.63E+12	1.58E+12	1.49E+12	1.55E+12
G8	1.53E+12	1.66E+12	1.55E+12	1.70E+12
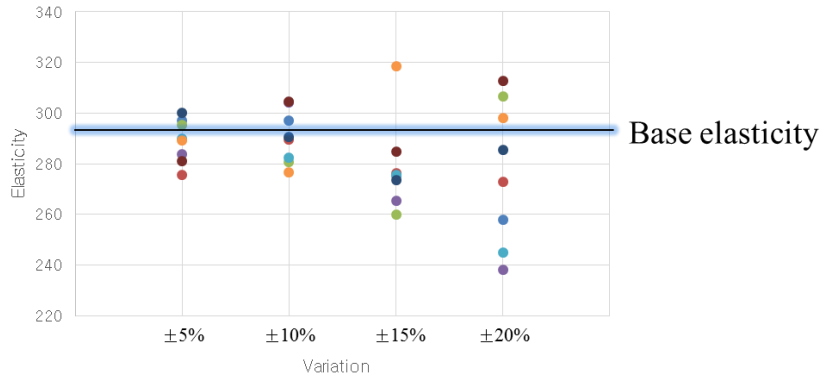
Figure 3. 24 Probabilistic distribution of the elasticity of the girder

3.6.2 Formulation of Objective Functions

As shown in Table 3.29, four different objective functions for the optimization process are constructed differently to ensure the generality of the proposed method. The objective function for the first case consists of the errors of the natural frequencies and uses both the RGD and the RGDAC from the second lane load with 5% variation. The objective function for the second case comprises the errors of the natural frequencies and uses both the RGD and the RGDAC from the second lane load with 10% variation. The objective function for the third case consists of the errors of the natural frequencies and uses both the RGD and the RGDAC from the second lane load with 15% variation. The objective function for the fourth case consists of the errors of the natural frequencies and uses both the RGD and the RGDAC from the second lane load with 20% variation

73

Table 3. 29 Objective functions used for the case study

	e_{NF}	e_{RGD}	e_{RGDAC}	Objective Function
Case 1	●	●	●	$\min J1(x) = \min(e_{NF} + e_{RGD} + e_{RGDAC})$
Case 2	●	●	●	$\min J_2(x) = \min(e_{NF} + e_{RGD} + e_{RGDAC})$
Case 3	●	●	●	$\min J_3(x) = \min(e_{NF} + e_{RGD} + e_{RGDAC})$
Case 4	●	●	●	$\min J_4(x) = \min(e_{NF} + e_{RGD} + e_{RGDAC})$

The objective function used to update the baseline FE model is composed of error functions, which are defined in chapter 2.2. The objective function for the discrepancies between the measured and analytical natural frequencies that uses the RGD and the RGDAC is given as Eq. (3.13):

$$\min J1\sim4(x) = \frac{1}{N}\sum_{j=1}^{N}\left(\frac{f(x)_j^a - f_j^m}{f_j^m}\right)^2 + \frac{1}{M}\sum_{i=1}^{M}\left(\frac{RGD(x)_i^a - RGD_i^m}{RGD_i^m}\right)^2 + \frac{\left(1-\sqrt{RGDAC}\right)^2}{RGDAC}$$

(3.13)

3.6.3 Comparison of Structural Responses

For cases 1 to 4, when the baseline FE model is updated using the RGD, the analytical values from the updated FE model and the measurement data are compared.

As shown in Table 3.30, the discrepancies in the natural frequencies increase as the variations in the flexural stiffness of the girder increase, and the updated FE model provides a similar discrepancy, which is shown in Fig. 3.25.

Table 3. 30 Discrepancies between the natural frequencies of the measured data and the updated FE model

	±5%	±10%	±15%	±20%
1 (B1)	0.023%	0.004%	-0.039%	0.585%
2 (T1)	-0.027%	-0.063%	-0.034%	-0.010%
3 (L1)	0.007%	-0.057%	0.060%	0.158%
4 (L2)	-0.227%	-0.128%	0.232%	0.084%
5 (T2)	0.020%	0.042%	0.183%	-0.358%
6 (C1)	-0.074%	0.004%	0.266%	-0.112%
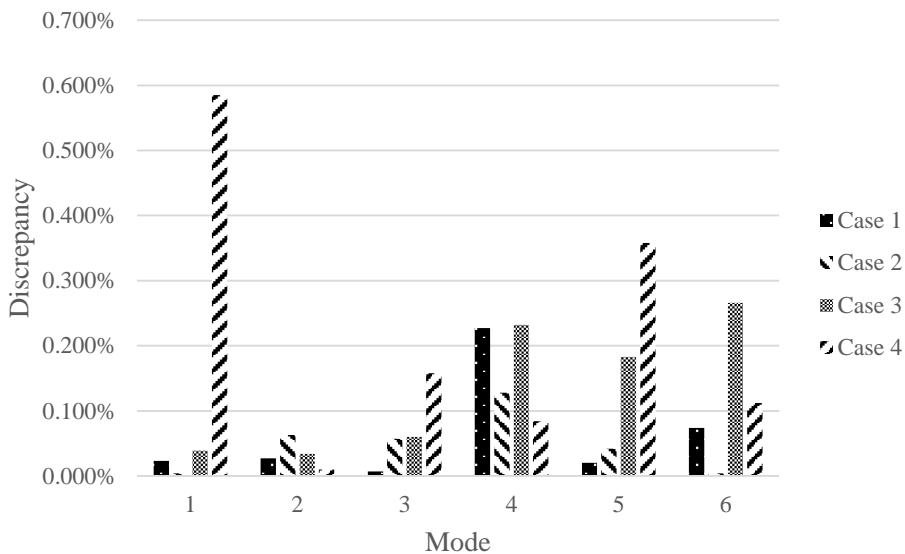
Figure 3. 25 Discrepancies between the natural frequencies of the measured data and the updated

Comparison of the updated static displacement results shown in Fig. 3.26 indicates that the discrepancy in the static displacement increases with larger variations in the girder's flexural stiffness.

The average displacement errors are 0.481%, 0.268%, 2.959%, and 3.053% for variations ranging from 5% to 20%. This case study has considered updates in the flexural stiffness of the girder that occur randomly. In the case study, the flexural

stiffness of the simulated bridge model was varied by 5 to 20%, and the differences

between the measured natural frequencies, mode shapes and vertical displacements

are then updated from the baseline FE model within the acceptable range.
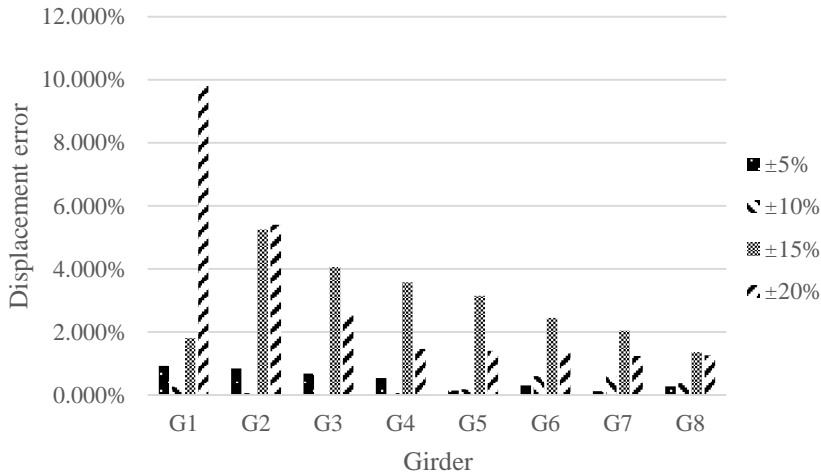
Figure 3. 26 Discrepancy between static displacements of the measured data and the
updated model cases

However, as the flexural stiffness distribution range of the girder broadens, the

improvement effect on the FE model is reduced. We will study the effects of this

deterioration in the improvement effect on the evaluation of the load-bearing rate in

Section 3.6.4.

3.6.4 Evaluation of Load Rating

The LRFR supports three limit states that follow the LRFD method. The service limit

state, the fatigue limit state and the strength limit state can therefore be evaluated as

load rating factors. In addition, the LRFR considers not only the designed load but

also the permitted load to check the safety of the bridge using the ADTT. The general

LRFR rating is given by Eq. (3.14):

$$RF = \frac{C - \gamma_{DC}DC - \gamma_{DW}DW \pm \gamma_p P}{\gamma_L LL(1+IM)} \qquad (3.14)$$

where C is the structural capacity, DC is the dead-load effect of the structural components, DW is the dead-load effect of the wearing surfaces and utilities, P is the permanent loading other than the dead loads, IM is the dynamic load allowance, and LL represents the live-load effect. The load factor γ_{DC} is applied to the weight of the structural components, the load factor γ_{DW} is applied to the wearing surfaces and utilities, the load factor γ_p is applied to any permanent loads other than the dead loads, and the load factor γ_L is applied to the live-load. Those load factors again follow the guidelines of the Manual for Bridge Evaluation (2008, AASHTO), as shown in Table 3.31.

Table 3. 31 Load factors used for evaluation of the load rating

γ_{DC}	γ_{DW}	γ_p	IM
1.25	1.50	1.75	0.174

Table 3. 32 Evaluated true load ratings and locations

	Case 1	Case 2	Case 3	Case 4
Load rating	1.981	1.989	1.817	1.764
Location	Girder 6	Girder 7	Girder 4	Girder 2

Table 3. 33 Evaluated load ratings and locations

	Case 1	Case 2	Case 3	Case 4
Load rating	1.987	1.994	1.778	1.677
Location	Girder 2	Girder 6	Girder 4	Girder 2

Comparison of Table 3.32 and Table 3.33 shows that when the flexural stiffness distribution of each girder is relatively small, the load rating values approximately match the true load rating values, but the girder positions used for evaluation of the load rating are different.

In contrast, when the flexural stiffness distribution is relatively large, the position of the girder used to evaluate the load rating is the same as the position for evaluation of the true load rating, but the difference between the load rating values is greater than in the small flexural stiffness distribution case. This can be seen in the same context as the load rating values and evaluated positions in the case where the stiffness of one girder is particularly low, as discussed in Section 3.4.

3.7 Summary

In this study, a frame model is constructed based on the sophisticated FE model that was used in the numerical evaluation. The bending stiffness value of the constructed frame model is varied arbitrarily, the structural response values are then analyzed as measurement data, and the optimization is applied to the baseline FE model to verify the proposed method. In addition, to generalize the proposed method, it is applied to the cases in which one inner girder is deteriorated, both inner and outer girders are deteriorated, and the girder deterioration is irregular. The effect of updating the FE model was confirmed by comparing the structural responses and the evaluated load ratings with the simulated true values.

The data that were measured in the field tests provide a variety of information on the behavior of the actual bridge. Using this information, the updated FE model shows bridge behavior that is similar to that of actual bridges, and the bridge performance can then be evaluated using structural parameter values with such behavior. One important point to consider when updating the FE model is that sufficient structural parameters must be used to describe the bridge behavior because updating of the FE model is an optimization problem intended to find structural parameter values that minimize the mismatch between measured and analytical structural responses. However, if there are too many structural parameters, the FE model considered here may not be optimized correctly. In addition, if there are too few structural parameters, the FE model may not be able to express the structural behavior of the actual structure. Therefore, a sensitivity check before the FE model update forms an important part of the update process.

Through a case study, it was confirmed that updating of the baseline FE model using both the static and dynamic measurement data produces results that are the closest to the actual bridge measurement data. Also, it was confirmed that the natural frequencies and the mode shape differences can be updated using the dynamic measurement data alone, but the minimization of the vertical displacement difference is less than that when the objective function consists of both the static and dynamic measurement data. However, when the relative displacement of the girder is used rather than the static displacement in the proposed method, it is confirmed that the limitations of using only the dynamic measurement data can be overcome using the RGD.

In addition, when the flexural stiffness values of several inner and outer girders are relatively low when compared with the other girders, use of all the static and dynamic measurement data to update the baseline FE model yields the closest results to the bridge measurement data. It is also possible to update the discrepancies in the natural frequencies and mode shapes using only the dynamic measurement data, but the minimization of the vertical displacement difference is less than that produced when the objective function is configured using both the static and dynamic error functions. However, when the relative displacement of the girder is used rather than the static displacement in the proposed method, it was found that the limitation of using the dynamic measurement data alone can be overcome using the RGD.

Finally, the flexural stiffness values of the simulated bridge model were varied by 5 to 20%, and the differences between the measured natural frequencies, mode shapes and vertical displacements are updated from those of the baseline FE model within the acceptable range. However, as the flexural stiffness distribution range of the girder broadens, the improvement effect of the FE model is reduced simultaneously. We then considered the effects of this deterioration in the improvement effect on the evaluation of the load-bearing rate.

Chapter 4. Application Example for a Real Bridge Structure

This chapter presents a numerical application of the proposed method to the Yeondae Bridge. Unlike the case of the simulated numerical example, the true values of the structural parameters of this bridge are unknown. Therefore, it is difficult to say definitively that the updated FE model is the only true solution because the result of updating the finite element model is the inverse problem to finding the structural parameters for the model that produce the most similar analytical values when compared with the measured data.

In this chapter, the proposed method is verified by comparing the evaluated load rating factor and the structural responses using the updated FE model. The effectiveness of the proposed method is verified through a case study, in which the model is updated using different objective functions based on the assumption of available measurement data.

4.1 General Description of Yeondae Bridge

The Yeondae Bridge was built in 2002 by the Korea Expressway Corporation (KEC) as part of an expressway in a test road section located alongside the main expressway. The bridge is usually closed to traffic but is occasionally opened for test purposes. The ultimate strength design (USD) process was applied to the design of the concrete slab, while the allowable stress design (ASD) procedure was used for design of the

steel box girder. Skewed abutments and internal piers support the bridge superstructure.

The bridge is composed of composite steel box girders with two box structures, as shown in Fig. 4.1. The bridge consists of four continuous spans that are each 45 m in length, as shown in Fig. 4.2. The concrete slab is composed of two lanes for a single direction with a net width of 11.7 m between the two side barriers.

Figure 4. 1 Yeondae Bridge (Kim, 2014)
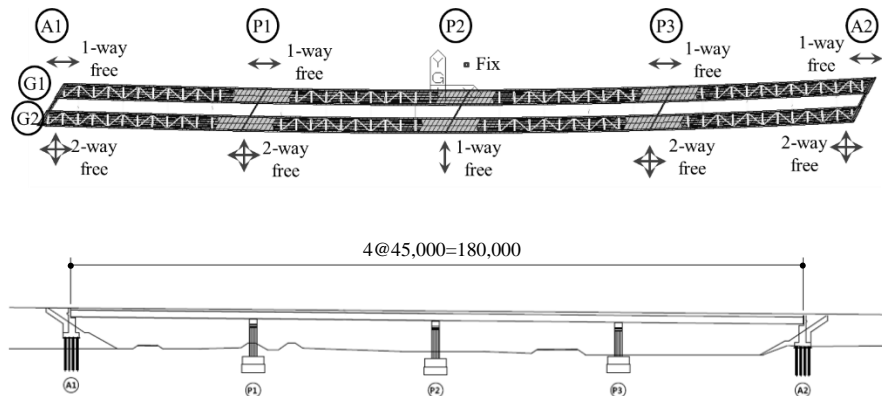
Figure 4. 2 Plane and side view of Yeondae Bridge (Kim, 2014)

4.2 Field Loading Tests

On March 31, 2013, static and dynamic loading tests were performed to determine the structural characteristics of the external loads. Two loaded trucks, which are shown in Figure 4.3, were used as the external loads and had weights of 260 kN each. Four displacement transducers were installed under the web plate of each box girder in the middle of the first span, as shown in Figure 4.4. Two static load cases and two dynamic load cases were considered in this procedure
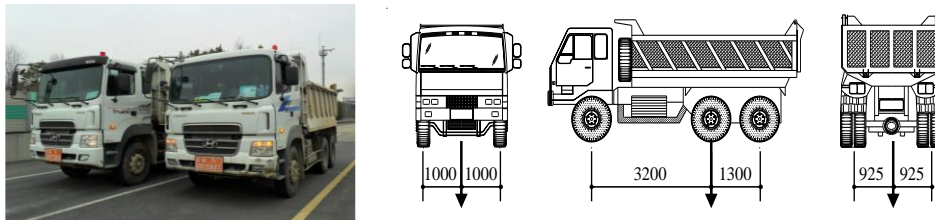
Figure 4. 3 Description of test trucks (Kim, 2014)
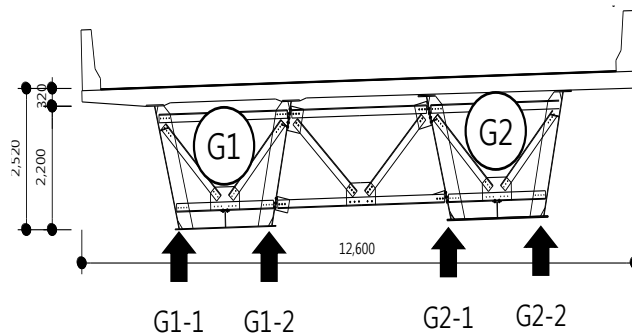
Figure 4. 4 Location of four displacement transducers (Kim, 2014)

In the static loading tests, a sensor that was suitable for use in the measurements was installed at a pre-selected point and the test vehicle was loaded to measure the vertical displacement that occurred at the measurement point. At this

stage, the positions at which the various sensors were installed and the load position of the test truck become the maximum response generation sites. The sensor installation positions are shown in Fig. 4.4 and the test truck load position is shown in Fig. 4.5. In the first static loading test, a single truck was placed in the first lane. In the second static loading test, single trucks were placed in the first lane and the second lane. The vertical displacement results that were measured with respect to the static loading are shown in Table 4.1. The static loading tests were performed three times at each loading position and the mean value obtained was then used as measurement data to update the FE model (Kim et al. 2013b).
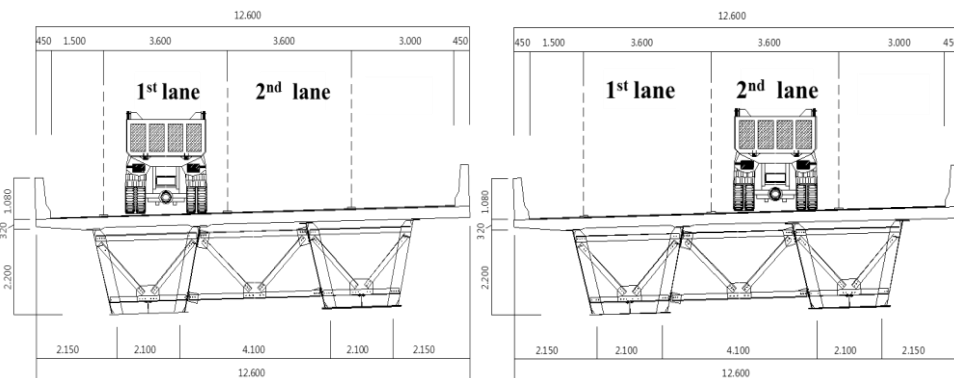
Figure 4. 5 Static loading Cases (Korea Concrete Institute [KCI], 2012)

Table 4. 1 Vertical displacements produced by the static load cases

	1st lane load case (mm)				2nd lane load case (mm)			
	1	2	3	Avg.	1	2	3	Avg.
G1-1	3.361	3.33	3.326	3.339	2.22	2.208	2.194	2.207
G1-2	3.236	3.205	3.191	3.211	2.718	2.714	2.716	2.716
G2-1	2.306	2.287	2.28	2.291	3.351	3.315	3.332	3.333
G2-2	1.938	1.914	1.908	1.920	3.142	3.119	3.125	3.129

Understanding of the dynamic behavior of bridges when vehicles are driven across them is crucial to assessment of the limits of resistance, stiffness, and serviceability of actual bridges. For this purpose, dynamic running tests were carried out to derive the basic data required for evaluation of the stability and usability of the target bridges by estimation of the dynamic effects and dynamic characteristics produced by running of the test vehicle. The dynamic driving tests were performed in the same locations in the lanes that were used in the static tests, as shown in Figure 4.5, and the truck speed was 10 km/h. The vertical displacements that were measured with respect to the dynamic loading are shown in Table 4.1. Each dynamic test was performed three times to ensure the reliability of the test results, which are given in Table 4.2 (Kim et al. 2013b).
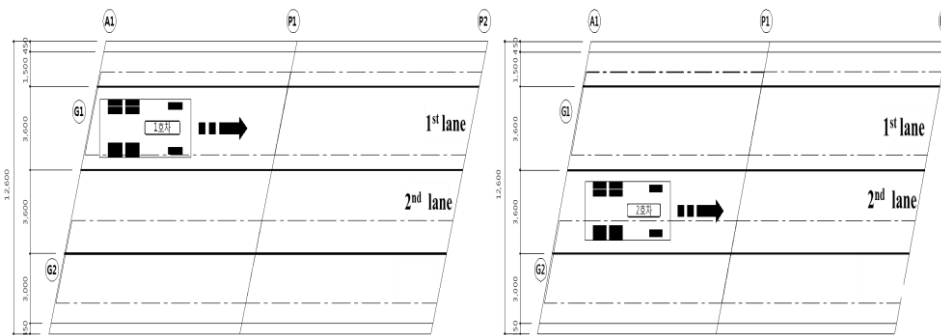
Figure 4. 6 Dynamic loading Cases (Korea Concrete Institute [KCI], 2012)

Unlike the static displacements, the dynamic displacements are produced by the superposition of signals at various frequencies. Therefore, the measured dynamic displacements have low-frequency components, which are displacements caused by movement of the load, and high-frequency components, which are affected by the interaction between the bridge and the vehicle.

Low-pass filtering can be adopted to separate the signals of various frequencies by eliminating the high-frequency components and retaining only the low-frequency components. The resulting signals are expected to represent the pseudo-static displacements induced by the loading of the truck weight, as shown in Figure 4.5 (Koh, 2014). The peak values of the filtered displacements could thus be regarded as the static displacements, as shown in Table 4.2.

The absolute magnitude of the maximum displacement is not exactly the same as the static displacement. However, the RGD still provides useful information that represents the relative ratio, and the advantage of using the RGD is that it can be obtained from a moving truck, meaning that traffic control is not necessary. In this research, the speed of the moving truck was set at 10 km/h, which is a comparatively slow speed, to allow the relationship between updating of the FE model and the RGD to be seen clearly by minimizing the effects of dynamic impacts.

(a) G1-1	(b) G1-2
(c) G2-1	(d) G2-2
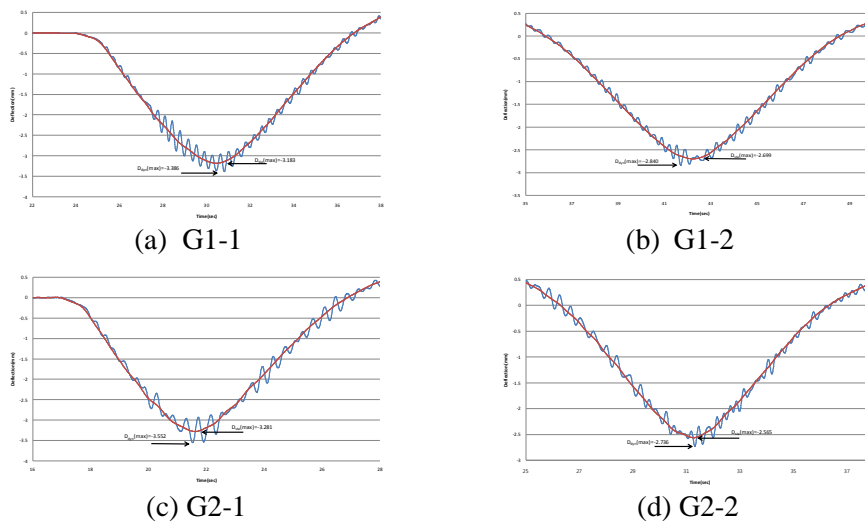
Figure 4. 7 Low pass filtering for evaluating max displacement   (Korea Concrete Institute [KCI], 2012)
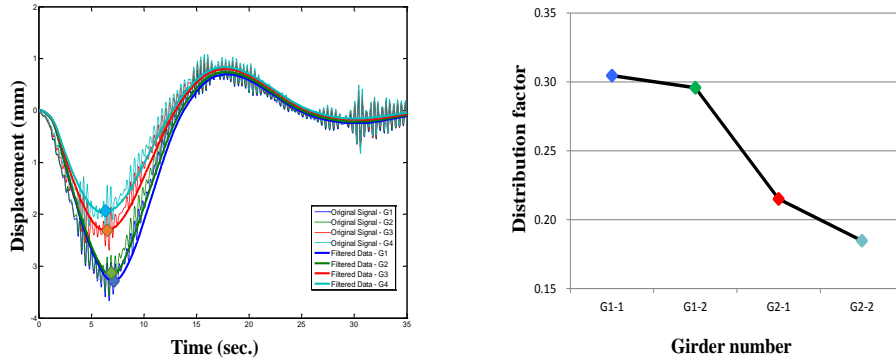
Figure 4. 8 Plotting of dynamic displacements measured at adjacent girders simultaneously (Kim, 2012)

Table 4. 2 Vertical displacement by the dynamic load cases

	1st lane load case (mm)				2nd lane load case (mm)			
	1	2	3	Avg.	1	2	3	Avg.
G1-1	3.277	3.33	3.287	3.298	2.204	2.222	2.218	2.215
G1-2	3.183	3.204	3.182	3.19	2.702	2.699	2.697	2.699
G2-1	2.314	2.33	2.319	2.321	3.281	3.286	3.313	3.293
G2-2	1.989	1.98	1.967	1.979	3.097	3.12	3.137	3.118

Both static and dynamic test was repeated three times in order to obtain reliable test results. The mode-shapes and associated natural frequencies for the first three modes are depicted in Figure 4.9 with the mode-shape obtained from an analytic model. Details about the experiments and findings have been summarized in Kim *et al*. (2013).

(a) 1st mode (2.32Hz)   (b) 2nd mode (2.61Hz)   (c) 3rd mode (3.42Hz)
Figure 4. 9 Mode-shape identified from the measured acceleration (Kim, 2014)
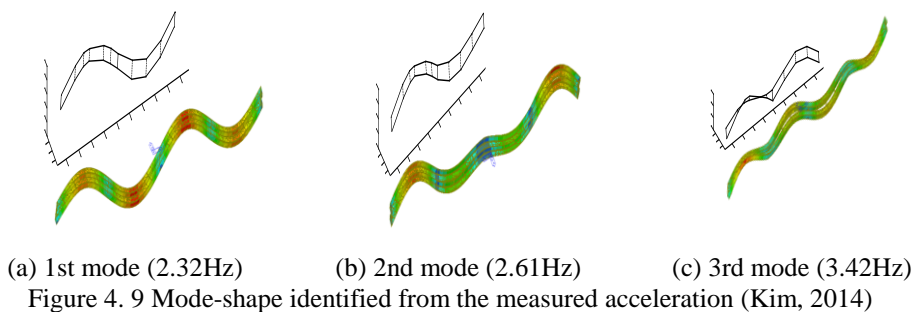
4.3 Development of the Baseline Finite Element Model

The Yeondae Bridge is modeled using the SAP2000 finite element analysis software, as shown in Fig. 4.10, based on the design specification. The box girders and the cross-beams are modeled using frame elements. Each box girder is simulated as a three-dimensional frame element. The equivalent cross-sectional area of a single box girder is calculated while considering the composite concrete deck. The stiffness of the cross-frame is calculated by taking the area of the concrete deck and the cross-bracing and framing between the two box girders into account.

Because the shell-frame FE model has fewer structural parameters than the sophisticated FE model, it has the advantage of reduced computation time when solving the optimization problem to minimize the differences between the measurement data and the analytically obtained values.
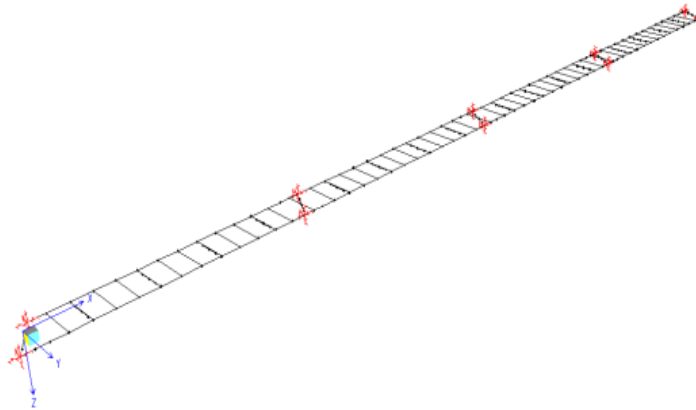
Figure 4. 10 Baseline FE model

4.4 Finite Element Model Updating Using the Proposed Method

4.4.1 Selection of Optimization Parameters

The first step towards solving the optimization problem is to determine the structural parameters. The optimization parameters must include the most important structural parameters. Simultaneously, it is also recommended that the total number of parameters used is equal to or less than the number of measurement data to avoid rank deficiency. A total of 61 structural parameters is preselected for this purpose, and include the density, the modulus of elasticity, the moment of inertia, the torsional stiffness and the spring coefficients for the supports. The structural parameters of the two girders are considered to be independent for each span. The preliminary analysis items are subdivided and grouped in terms of their importance and relevance in the following analyses.

Four steps are proposed to determine effective structural parameters that are clearly related to the behavior of the multiple girder bridge. The first step involves creation of 100 random FE models based on the baseline FE model. The second step is to perform a sensitivity check by evaluating the errors in the static displacements and natural frequencies for each random model. The discrepancies between the measured and analytical natural frequencies and static displacements are given as Eq (4.1) and Eq. (4.2) below:

$$e(x)_f = \frac{1}{N}\sum_{j=1}^{N}\left(\frac{f(x)_j^a - f_j^m}{f_j^m}\right)^2 \tag{4.1}$$

$$e(x)_\delta = \frac{1}{M} \sum_{i=1}^{M} \left(\frac{\delta(x)_i^a - \delta_i^m}{\delta_i^m} \right)^2 \qquad (4.2)$$

Here, $e(x)_f$ is the residual error of the natural frequency, f_j is the j-th natural frequency (where $j=1$ – number of natural frequencies), $e(x)_\delta$ is the residual error of the static displacement, δ_i is the vertical displacement of the i-th girder (where $i=1$ – number of girders) and the superscripts a and m represent values from the FE model analysis and the measured data, respectively. The third step is to characterize the structural parameters by application of a principal component analysis (PCA) to the sensitivity matrix. The analyzed structural variables are as shown in Figure 4.11, where the vector length represents the importance of the structural parameter in selection of the structural parameters based on the bridge behavior, and the vector direction represents the structural parameter characteristics for grouping of parameters with similar characteristics. The final step is then to select the most important structural parameters to describe the bridge behavior and to group the structural parameters with similar characteristics together.

A total of 61 structural parameters that can represent the complex behavior of a steel box girder bridge were preselected. Finally, using the characteristics of the structural variables from analysis, the structural variables with similar sensitivities were grouped together and small sensitivity characteristics were reduced in terms of the location of the structural member. 37 structural variables, which are based on eight variables including the mass, the elasticity, the torsional stiffness, the moment of inertia, and the area of the transverse slab in terms of the four spans, were selected as shown in Table 4.3. The optimal structural parameters were then identified by

90

sequential quadratic programming (SQP). As a result, the updated FE model shows errors of less than 5% for the summation of the static displacements and between the natural frequencies of the measured data and the analytical values.
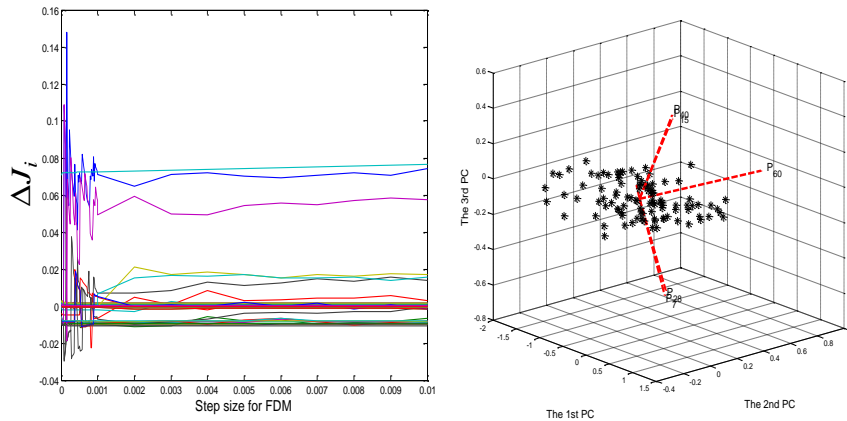
Figure 4. 11 Selection of structural parameter by PCA

Table 4. 3 Structural parameters and their allowable bounds considered in the optimization

Structural parameters	Allowable bounds (%)
Coefficients of spring support elements in translation and rotational direction	±30
Mass of girders (span 1, 2, 3 and 4), cross frame	±10
Young's modulus of girders (span 1, 2, 3 and 4), cross frame, and slab	±20
Torsional stiffness of girders (span 1, 2, 3 and 4),cross frame, and slab	±25
Moment of inertia (I_{yy})of girders (span 1, 2, 3 and 4), cross frame, and slab	±10
Moment of inertia (I_{zz})of girders (span 1, 2, 3 and 4), cross frame, and slab	±10
Area of transverse slab	±30
Mass of substructural member (vertical, rotational)	±30

4.4.2 Formulation of Objective Functions

As shown in Table 4.4, five different objective functions for the optimization process are constructed differently to ensure the generality of the proposed method. The objective function in the first case consists of the natural frequencies and the MAC when the bridge traffic could not be controlled and the FE model is updated using only the dynamic measurement data. The objective function in the second case consists of the natural frequency, the MAC, and the static displacement when a single truck is loaded on the first lane, and the FE model is updated using both static and dynamic measurement data obtained through traffic control on the bridge. The objective function used for the third case consists of the natural frequency, the MAC, and the static displacement when a single truck is loaded on the second lane. The objective function in the fourth case consists of the errors of the natural frequencies and both the RGD and the RGDAC when a moving truck is loaded on the first lane. Finally, the objective function used in the fifth case consists of the errors of the natural frequencies and both the RGD and the RGDAC when the moving truck is loaded in the second lane.

Table 4. 4 Objective functions used for the case study

Case	e_{NF}	e_{MAC}	e_{DISP}	e_{RGD} e_{RGDAC}	Objective Function
1	●	●			$min\,J1(x) = min(e_{NF} + e_{MAC})$
2	●	●	●		$min\,J2(x) = min(e_{NF} + e_{MAC} + e_{DISP}^{1st})$
3	●	●	●		$min\,J3(x) = min(e_{NF} + e_{MAC} + e_{DISP}^{2nd})$
4	●			●	$min\,J4(x) = min(e_{NF} + e_{RGD}^{1st} + e_{RGDAC}^{1st})$
5	●			●	$min\,J5(x) = min(e_{NF} + e_{RGD}^{2nd} + e_{RGDAC}^{2nd})$

The objective function used to update the baseline FE model is composed of error functions, which are defined in Chapter 2.2. The objective function used to determine the discrepancies between the measured and analytical natural frequencies and the MAC values is given as Eq. (4.3):

$$min\,J1(\text{x}) = \frac{1}{N}\sum_{j=1}^{N}\left(\frac{f(x)_j^a - f_j^m}{f_j^m}\right)^2 + \frac{1}{N}\sum_{j=1}^{N}\frac{\left(1 - \sqrt{MAC_j}\right)^2}{MAC_j} \tag{4.3}$$

The objective function used for the discrepancies between the measured and analytical natural frequencies and the static displacements is given as Eq. (4.4):

$$min\,J2{\sim}3(\text{x}) = \frac{1}{N}\sum_{j=1}^{N}\left(\frac{f(x)_j^a - f_j^m}{f_j^m}\right)^2 + \frac{1}{M}\sum_{i=1}^{M}\left(\frac{\delta(x)_i^a - \delta_i^m}{\delta_i^m}\right)^2$$

$$\tag{4.4}$$

The objective function used for the discrepancies between the measured and analytical natural frequencies using the RGD and the RGDAC is given as Eq. (4.5).

Each case has the same objective function, but different RGD and RGDAC values are used, which are dependent on the location of the lane load.

$$min\,J4{\sim}5(\text{x}) = \frac{1}{N}\sum_{j=1}^{N}\left(\frac{f(x)_j^a - f_j^m}{f_j^m}\right)^2 + \frac{1}{M}\sum_{i=1}^{M}\left(\frac{RGD(x)_i^a - RGD_i^m}{RGD_i^m}\right)^2 + \frac{\left(1 - \sqrt{RGDAC}\right)^2}{RGDAC}$$

(4.5)

4.5 Bridge Performance Evaluation

4.5.1 Comparison of the Structural Responses

Table 4.5 shows that the discrepancies between the natural frequencies from the measurement data and those from the updated FE models are minimal, as illustrated in Fig. 3.20. The updated results show similar trends that are dependent on how each objective function is configured. The difference between the measured value and the analytical value of the natural frequency was at its lowest when the objective function was optimized using only the dynamic measurement data (case 1), such as the natural frequency and the MAC. In contrast, when the optimization process is performed using the dynamic measurement data (cases 4 and 5), the objective function is the natural frequency and the proposed method uses the RGD and the RGDAC, the natural frequency difference between the measured and analytical values is at its highest, as shown in Fig. 4.10. The objective function consisting of the natural frequency and the static displacement provides the median updated results.

Table 4. 5 Natural frequencies from the measured data and the updated FE mode

Mode No.	Measured frequency (Hz)	Case 1 (Hz)	Case 2 (Hz)	Case 3 (Hz)	Case 4 (Hz)	Case 5 (Hz)
1 (B1)	2.319	2.319	2.338	2.293	2.285	2.274
2 (T1)	2.612	2.612	2.617	2.613	2.644	2.607
3 (L1)	3.418	3.418	3.384	3.423	3.431	3.479
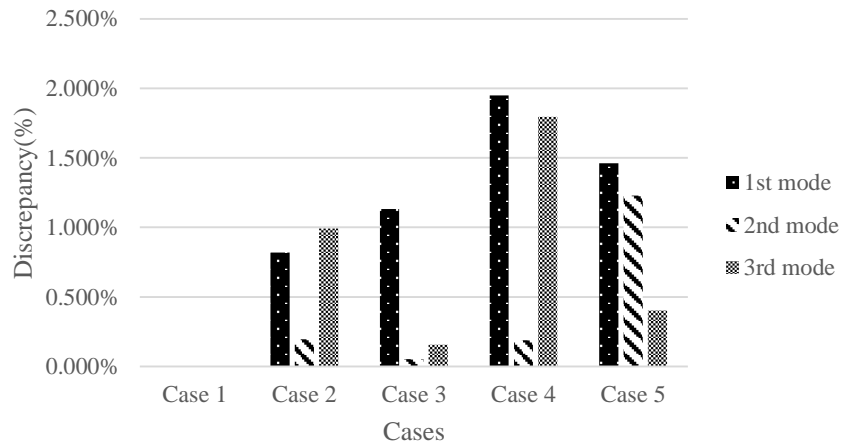
Figure 4. 12 Discrepancies between the natural frequencies of the measured data and the updated model cases

As shown in Fig. 4.13, the static displacement result from the updated FE model showed the greatest improvement effect when the FE model was updated using both the static and dynamic measurement data (cases 2 and 3). Therefore, the FE model that was updated by the proposed method (cases 3 and 4) provided better improvement effects than the objective function that uses the dynamic measurement data only (case 1).
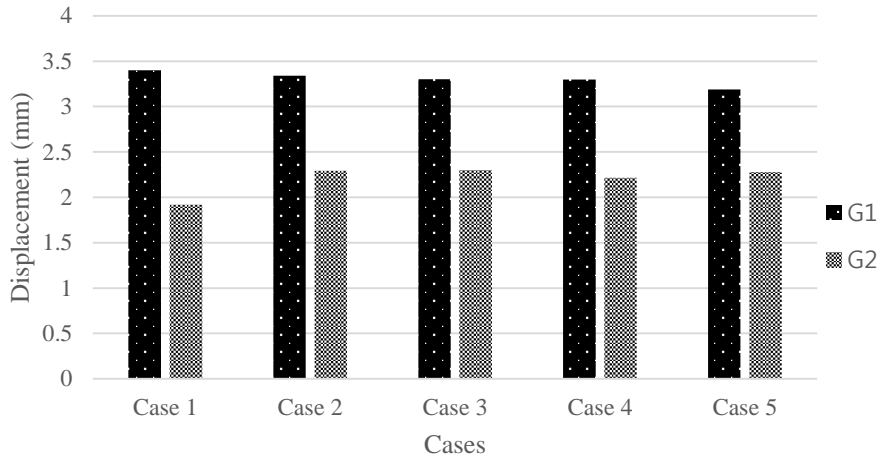
Figure 4. 13 Discrepancies between the static displacements of the measured data and the updated model cases

This case study has also demonstrated updating of the FE model using the example of a real bridge, the Yeondae Bridge, using the field test data. The updated results show that is possible to update any discrepancies in the natural frequency and the mode shapes using only the dynamic measurement data, but it was also found that the difference in the vertical displacement was minimized to a lesser degree than when the objective function was configured using both the static and dynamic error functions. Use of all the static and dynamic measurement data to update the baseline FE model yields the closest results to the actual bridge measurement data. However, when the relative displacement of the girder was used rather than the static displacement in the proposed method, it was found that the limitations of use of dynamic measurement data only can be overcome using the RGD.

4.5.2 Evaluation of Load Rating

The LRFR supports three limit states that follow the LRFD method. The service limit state, the fatigue limit state and the strength limit state can therefore be evaluated as rating factors. In addition, the LRFR considers not only the designed load but also the permitted load to check the safety of the bridge using the ADTT. The general LRFR rating is given by Eq.(4.6):

$$\text{RF} = \frac{C - \gamma_{DC} DC - \gamma_{DW} DW \pm \gamma_p P}{\gamma_L LL(1+IM)} \tag{4.6}$$

Here, C is the structural capacity, DC is the dead-load effect of the structural components, DW is the dead-load effect of the wearing surfaces and utilities, P represents the permanent loading other than the dead loads, IM represents the dynamic load allowance, and LL is the live-load effect. The load factor γ_{DC} is applied to the weights of the structural components, the load factor γ_{DW} is applied to the wearing surfaces and utilities, the load factor γ_p is applied to any permanent loads other than the dead loads, and the load factor γ_L is applied to the live-load. These load factors follow guidance of the Manual for Bridge Evaluation (2008, AASHTO), as shown in Table 3.26.

Table 4. 6 Load factors used for evaluation of the load rating

γ_{DC}	γ_{DW}	γ_p	IM
1.25	1.50	1.75	0.174

Table 4. 7 The evaluated load rating

	Case 1	Case 2	Case 3	Case 4	Case 5
Load rating	3.2141	2.5578	2.6949	2.3414	2.8867

As shown in Table 4.7, the evaluated load rating derived using the proposed method (cases 4 and 5) shows similar results to cases 2 and 3 with regard to value and location. When the objective function consists of the RGD and the RGDAC with the natural frequencies, it provides the same girder location as that of cases 2 and 3 for evaluation of the load rating and shows similar load rating values. In contrast, the objective function consisting of the natural frequencies and the mode shapes shows a larger load rating value when compared with cases 4 and 5 and cases 2 and 3, even if it provides the same girder location for evaluation of the load rating.

4.6 Summary

This chapter presents a numerical application of the proposed method to the Yeondae Bridge. Unlike the simulated numerical example, the true values of the structural parameters of this bridge are unknown. Therefore, it is difficult to conclude that the updated FE model is the only true solution because the updated result of the FE model is the inverse problem to determination of the structural parameters of the model with analytical values that are most similar to the measured data.

Updating of the model of the Yeondae Bridge example using the field test data provides the updated results from which it is possible to update any discrepancies in the natural frequencies and the mode shapes using only the dynamic measurement data; however, it was found that the differences in the vertical displacement were minimized to a lesser degree than when the objective function was configured using both static and dynamic error functions. Use of all the static and dynamic

98

measurement data to update the baseline FE model yields results that are closest to the bridge measurement data. However, when the relative displacement of the girder is used rather than the static displacement in the proposed method, it was found that the limitations of using only the dynamic measurement data can be overcome using the RGD

Chapter 5. Conclusion

This work has proposed a new method to update a finite element (FE) model of a bridge using ambient vibration data. While ambient vibration data are advantageous from a data collection perspective, they are restricted to provision of global level information. Therefore, updating of models using these data often leads to a lack of accuracy, particularly in calculations of the load rating factor (RF). In this study, the relative girder displacement (RGD) and the relative girder displacement assurance criterion (RGDAC) were used as indices to update FE models. Because they have been acquired from dynamic displacement data, the RGD and the RGDAC are expected to contain local level information that is implicitly similar to the static displacement data. These two indices were embedded into the objective function for optimization that was used in the FE model update procedure.

To investigate the influence of the objective function on the model update accuracy, various objective functions were formulated using different combinations of variables and the corresponding updated models were then analyzed for comparison. The results of comprehensive numerical investigations using simulated bridge models with different sets of damage and loading locations and a real bridge model has proved that the optimal form of the objective function with the RGD and the RGDAC provides more accurate results for updating of the FE model in a more efficient manner than other updating methods that use ambient vibration data. The following findings were drawn from numerical investigations of the simulated bridge

models.

- When the objective function contains either the RGD term or the RGDAC term alone, it was difficult to find a solution (for the girder stiffness) because the problem is a typically ill-posed problem. For example, an RGDAC-only problem often yielded a model that showed a deflection shape that was similar to that of the exact solution, but the deflection values generated were quite different.

- When the objective function contained both the RGD and RGDAC terms, it always converged to produce fairly accurate solutions to the problems considered in this study. It was inferred that the RGD and the RGDAC play roles in supplementing each other to find not only the deflection shape but also the absolute deflection values. Updating the FE model using this combination also led to a much more exact model when compared with a model that was updated using the mode shape and the natural frequency, which has been a typical method for use of ambient vibration data.

- The location of the loading does not seem to affect the updating of the FE model by the proposed method. When both the RGD and the RGDAC were used for the objective function, updating of the FE model consistently resulted in feasible solutions, regardless of the location of the traffic lane.

The proposed method was also applied to an existing bridge that had been examined thoroughly in field loading tests. After a baseline FE model of this bridge had been created, the model was updated successfully using only the dynamic data.

The RF of the bridge was also evaluated as an illustrative example for practical applications.

The proposed method is capable of improving the accuracy of the updated FE model using only the ambient vibration data. As a powerful model updating tool for use when only limited data are available, this method can contribute to the integrated maintenance of numerous bridges in operation without the need for any traffic control. However, there are many different uncertainties in reality in areas such as data measurement and model composition that were considered to be deterministic in this study. For a realistic analysis, the effects of these uncertainties on the RGD and the RGDAC and on consequent updates to the FE models must be investigated further.

.

References

김현수, 김유희, 박종칠 & 신수봉, 2013. 서해대교 건전성 모니터링을 위한 데이터 분석 및 건전성지수. *대한토목학회논문집*, 33 (2), 387-395.

박원석, 2017. *교량의 유한요소 모델 업데이팅 최신 기술*. 2016 건설기술연구사업 <상시 센서 데이터를 활용한 케이블 교량 운용중 업데이팅 기술 개발> 과제 보고서.

박용명, 백승용 & 황민오, 2002. 강합성 플레이트거더교의 가로보 배치에 관한 연구. *한국강구조학회 논문집*, 14 (6), 691-699.

Agbabian, M., Masri, S., Miller, R. & Caughey, T., 1991. System identification approach to detection of structural changes. *Journal of Engineering Mechanics*, 117 (2), 370-390.

Aktan, A.E. & Farhey, D.N., 1996. *Condition and reliability assessment of constructed facilities*. Special Publication, American Concrete Institute, 162, 73-92.

Aktan, A.E., Farhey, D.N., Helmicki, A.J., Brown, D.L., Hunt, V.J., Lee, K.-L. & Levi, A., 1997. Structural identification for condition assessment: Experimental arts. *Journal of Structural Engineering*, 123 (12), 1674-1684.

Aktan, A.E., atbaş, N., Türer, A. & Zhang, Z., 1998. Structural identification: Analytical aspects. *Journal of Structural Engineering*, 124 (7), 817-829.

Allemang, R.J. & Brown, D.L., 1982. A correlation coefficient for modal vector analysis. *Proceedings of the 1st international modal analysis conference*, Orlando: Union College Press, 110-116.

Allemang, R.J., 2003. The modal assurance criterion–twenty years of use and abuse. *Sound and vibration*, 37 (8), 14-23.

Bagchi, A., 2005. Updating the mathematical model of a structure using vibration data. *Journals of Vibration and Control,* 11 (12), 1469-1486.

Barker, R.M. & Puckett, J.A., 2013. *Design of highway bridges: An LRFD approach.* Hoboken, NJ: John wiley & sons.

Bell, E.S., Sanayei, M., Javdekar, C.N. & Slavsky, E., 2007. Multiresponse parameter estimation for finite-element model updating using nondestructive test data. *Journal of Structural Engineering,* 133 (8), 1067-1079.

Bergmeister, K. & Santa, U. 2000. Global mentoring concepts for bridges. In: Nondestructive Evaluation of Highways, Utilities, and Pipelines IV, SPIE, Bellingham, WA, 3995, 4-25.

Bernard, K.J., Culmo, M.P. & Dewolf, J.T., 1997. Strain monitoring to evaluate steel bridge connections. *Building to Last*, ASCE, 919-923.

Brownjohn, J.M. & Xia, P.-Q., 2000. Dynamic assessment of curved cable-stayed bridge by model updating. *Journal of Structural Engineering,* 126 (2), 252-260.

Brownjohn, J.M., Xia, P.-Q., Hao, H. & Xia, Y., 2001. Civil structure condition assessment by fe model updating: Methodology and case studies. *Finite elements in analysis and design,* 37 (10), 761-775.

Brownjohn, J.M.W., Moyo, P., Omenzetter, P. & Lu, Y., 2003. Assessment of highway bridge upgrading by dynamic testing and finite-element model updating. *Journal of Bridge Engineering,* 8 (3), 162-172.

Bu, J., Law, S. & Zhu, X., 2006. Innovative bridge condition assessment from dynamic response of a passing vehicle. *Journal of Engineering Mechanics,* 132 (12), 1372-1379.

Cardini, A. & Dewolf, J.T., 2009. Long-term structural health monitoring of a multi-girder steel composite bridge using strain data. *Structural Health Monitoring*, 8 (1), 47-58.

Catbas, F.N. & Aktan, A.E., 2002. Condition and damage assessment: Issues and some promising indices. *Journal of Structural Engineering,* 128 (8), 1026-1036.

Catbas, F.N., Ciloglu, S.K., Hasancebi, O., Grimmelsman, K. & Aktan, A.E., 2007. Limitations in structural identification of large constructed structures. *Journal of Structural Engineering,* 133 (8), 1051-1066.

Catbas, F.N, Kijewski-Correa, T. & Aktan A.E., 2011. *Structural Identification (St-Id) of Constructed Facilities*. A State-of-the Art Report, ASCE SEI Committee on Structural Identification of Constructured Systems, Virginia:ASCE.

Catbas, F.N., Susoy, M. & Frangopol, D.M., 2008. Structural health monitoring and reliability estimation: Long span truss bridge application with environmental monitoring data. *Engineering Structures*, 30 (9), 2347-2359.

Chajes, M.J., Mertz, D.R. & Commander, B., 1997. Experimental load rating of a posted bridge. *Journal of Bridge Engineering*, 2 (1), 1-10.

Chang, F.K. (ed.), 2001, *Structural health monitoring : the demands and challenges*. Proceedeings of the 3rd International Workshop on Structural Health Monitoring : the Demands and Challenges, Stanford University, CA.

Chang, M. & Pakzad, S.N., 2014. Optimal sensor placement for modal identification of bridge systems considering number of sensing nodes. *Journal of Bridge Engineering,* 19 (6), 04014019.

Daniell, W.E. & Macdonald, J.H., 2007. Improved finite element modelling of a cable-stayed bridge through systematic manual tuning. *Engineering Structures*, 29 (3), 358-371.

Deng, L. & Cai, C., 2009. Bridge model updating using response surface method and genetic algorithm. *Journal of Bridge Engineering,* 15 (5), 553-564.

DeWolf, J.T., Lauzon, R.G. & Culmo, M.P., 2002. Monitoring Bridge Performance. *Structural Health Monitoring Journal*, 1 (2), 129-138.

Denoyer, K.K. & Peterson, L.D., 1997. Method for structural model update using dynamically measured static flexibility matrices. *AIAA journal,* 35 (2).

Doebling, S.W., Farrar, C.R. & Prime, M.B., 1998. A summary review of vibration-based damage identification methods. *Shock and vibration digest,* 30 (2), 91-105.

Dubbs, N. & Moon, F., 2016. Assessment of long-span bridge performance issues through an iterative approach to ambient vibration–based structural identification. *Journal of Performance of Constructed Facilities,* 30 (5), 04016029.

Erdogan, Y.S., Gul, M., Catbas, F.N. & Bakir, P.G., 2014. Investigation of uncertainty changes in model outputs for finite-element model updating using structural health monitoring data. *Journal of Structural Engineering,* 140 (11), 04014078.

Farrar, C.R. & Worden, K., 2007. An introduction to structural health monitoring. *Philosophical Transactions of the Royal Society of London A: Mathematical, Physical and Engineering Sciences*, 365 (1851), 303-315.

Federal Highway Administration, 1995. *Recording and Coding Guide for the Structure Inventory and Appraisal of the Nation's Bridges*. Report FHWA-PD-96-001, Washington, D.C.:Department of Transportation.

Federal Highway Administration, 2011. *Visual Inspections and Field Tests for the Assessment of the Test-Bed Bridge of International Bridge Study – Final Report*. International Bridge Study (IBS) of Long-Term Bridge Performance (LTBP) Program (Korean Joint Team), Washington, D.C.:Department of Transportation.

Feng, M.Q., Kim, D.K., Yi, J.-H. & Chen, Y., 2004. Baseline models for bridge performance monitoring. *Journal of Engineering Mechanics,* 130 (5), 562-569.

Florida department of Transportation, 2015. *Bridge load rating manual*. Florida: FDOT.

Frangopol, D.M., Strauss, A. & Kim, S., 2008. Bridge reliability assessment based on monitoring. *Journal of Bridge Engineering*, 13 (3), 258-270.

Friswell, M. & Mottershead, J.E., 2013. *Finite element model updating in structural dynamics*: Springer Science & Business Media.

Garcia-Palencia, A.J., Santini-Bell, E., Sipple, J.D. & Sanayei, M., 2015. Structural model updating of an in-service bridge using dynamic data. *Structural Control and Health Monitoring,* 22 (10), 1265-1281.

Harris, D.K., 2010. Assessment of flexural lateral load distribution methodologies for stringer bridges. *Engineering Structures*, 32 (11), 3443-3451.

Hemez, F.M. & Doebling, S.W., 2001. Review and assessment of model updating for non-linear, transient dynamics. *Mechanical Systems and Signal Processing,* 15 (1), 45-74.

Huang, D., 2004. Field test and rating of arlington curved-steel box-girder bridge: Jacksonville, Florida. *Transportation Research Record: Journal of the Transportation Research Board*, (1892), 178-186

Huria, V., Lee, K.-L. & Aktan, A.E., 1993. Nonlinear finite element analysis of RC slab bridge. *Journal of Structural Engineering*, 119 (1), 88-107.

Jaishi, B. & Ren, W.-X., 2005. Structural finite element model updating using ambient vibration test results. *Journal of Structural Engineering,* 131 (4), 617-628.

Jang, J. & Smyth, A.W., 2017. Model updating of a full-scale fe model with nonlinear constraint equations and sensitivity-based cluster analysis for updating parameters. *Mechanical Systems and Signal Processing,* 83, 337-355.

Jang, S., Li, J. & Spencer Jr, B.F., 2012. Corrosion estimation of a historic truss bridge using model updating. *Journal of Bridge Engineering,* 18 (7), 678-689.

Jin, S.-S., Cho, S., Jung, H.-J., Lee, J.-J. & Yun, C.-B., 2014. A new multi-objective approach to finite element model updating. *Journal of Sound and Vibration,* 333 (11), 2323-2338.

Jonsson, F. & Johnson, D., 2007. Finite element model updating of the new svinesund bridge - Manual model refinement with non-linear optimization, Master's thesis in the International Master's Programme Structural Engineering, Department of Civil and Environmental Engineering, Chalmers University of Technology, Goteborg, Sweden.

Kayser, J.R. & Nowak, A.S., 1989. Capacity loss due to corrosion in steel-girder bridges. *Journal of Structural Engineering,* 115 (6), 1525-1537.

Kim, H.-J., Kim, H.-K. & Park, J.Y., 2013. Reliability-based evaluation of load carrying capacity for a composite box girder bridge. *KSCE Journal of Civil Engineering*, 17 (3), 575-583.

Kim, H.-J., Park, W., Koh, H.-M. & Choo, J.F., 2013. Identification of structural performance of a steel-box girder bridge using machine learning technique. *Proceeding of IABSE Symposium* 2013, 1313-1320.

Kim, H.-J., Park, W. & Koh, H.-M., 2014. Probabilistic performance assessment of highway bridges using operational monitoring data. *Proceeding of IABSE Symposium 2014*, 2650-2657.

Kim, H.-J., 2015. *Probabilistic assessment of structural condition through clustering-based multiple FE model update*. Doctoral dissertation, Department of Civil and Environmental Engineering, Seoul National University, Seoul, Korea.

Kim, H.-J., Kim, D.B. & Koh, H.-M., 2015. Condition Assessment of a Steel-box Girder Bridge through Finite Element Model Updating with Effective Parameters. *Proceeding of 8th International Symposium on Steel Structures*.

Koch, C., Georgieva, K., Kasireddy, V., Akinci, B. & Fieguth, P., 2015. A review on computer vision based defect detection and condition assessment of concrete and asphalt civil infrastructure. *Advanced Engineering Informatics,* 29 (2), 196-210.

Ko, J. & Ni, Y., 2005. Technology developments in structural health monitoring of large-scale bridges. *Engineering structures*, 27 (12), 1715-1725.

Ko, J., Ni, Y., Zhou, H., Wang, J. & Zhou, X., 2009. Investigation concerning structural health monitoring of an instrumented cable-stayed bridge. *Structures & Infrastructure Engineering*, 5 (6), 497-513.

Koh, H.M., Lee, H.S., Kim, S. & Choo, J.F., 2009. Monitoring of bridges in korea. *Encyclopedia of Structural Health Monitoring*, John Wiley & Sons.

Kodikara, K., Chan, T., Nguyen, T. & Thambiratnam, D., 2016. Model updating of real structures with ambient vibration data. *Journal of Civil Structural Health Monitoring,* 6 (3), 329-341.

Koshiba, A., Abe, M., Sunaga, T. & Ishii, H., 2001. Bridge inspection in steel road bridge based on real measurement. *Current and Future Trends in Bridge Design Construction and Maintenance*, 2, 268-273.

Korea Concrete Institute, 2012. *성능기반 교량안전성 평가기법 개발 및 검증*

용역 *(2차) 보고서*. (in Korean)

Kuhn, K.D. & Madanat, S.M., 2005. Model uncertainty and the management of a system of infrastructure facilities. *Transportation Research Part C: Emerging Technologies,* 13 (5), 391-404.

Levin, R. & Lieven, N., 1998. Dynamic finite element model updating using simulated annealing and genetic algorithms. *Mechanical Systems and Signal Processing*, 12 (1), 91-120.

Li, Z., Chan, T.H., Yu, Y. & Sun, Z., 2009. Concurrent multi-scale modeling of civil infrastructures for analyses on structural deterioration—part i: Modeling methodology and strategy. *Finite Elements in Analysis and Design,* 45 (11), 782-794.

Liu, C., Dewolf, J.T. & Kim, J.-H., 2009a. Development of a baseline for structural health monitoring for a curved post-tensioned concrete box–girder bridge. *Engineering Structures,* 31 (12), 3107-3115.

Liu, M., Frangopol, D.M. & Kim, S., 2009b. Bridge safety evaluation based on monitored live load effects. *Journal of Bridge Engineering,* 14 (4), 257-269.

Liu, M., Frangopol, D.M. & Kim, S., 2009c. Bridge system performance assessment from structural health monitoring: A case study. *Journal of Structural Engineering,* 135 (6), 733-742.

Macdonald, J.H. & Daniell, W.E., 2005. Variation of modal parameters of a cable-stayed bridge identified from ambient vibration measurements and fe modelling. *Engineering Structures,* 27 (13), 1916-1930.

Mašović, S. & Hajdin, R., 2014. Modelling of bridge elements deterioration for serbian bridge inventory. *Structure and Infrastructure Engineering,* 10 (8), 976-987.

Miyamoto, A., Kawamura, K. & Nakamura, H., 2000. Bridge management system and maintenance optimization for existing bridges. *Computer‑Aided Civil and Infrastructure Engineering,* 15 (1), 45-55.

MLTM, 2012. *Highway Bridge Design Code*, Korea Ministry of Land, Transportation and Maritime Affairs, Seoul, Korea.

Mohammed, M., Sulaeman, E. & Mustapha, F., 2017. Dynamic response for structural health monitoring of the penang (i) cable-stayed bridge. *IOP Conference Series: Materials Science and Engineering*, IOP Publishing, 012068.

Morassi, A. & Tonon, S., 2008. Dynamic testing for structural identification of a bridge. *Journal of bridge engineering,* 13 (6), 573-585.

Morcous, G., Rivard, H. & Hanna, A., 2002. Modeling bridge deterioration using case-based reasoning. *Journal of Infrastructure Systems,* 8 (3), 86-95.

Mottershead, J. & Friswell, M., 1993. Model updating in structural dynamics: A survey. *Journal of sound and vibration,* 167 (2), 347-375.

Mottershead, J.E., Link, M. & Friswell, M.I., 2011. The sensitivity method in finite element model updating: A tutorial. *Mechanical systems and signal processing*, 25 (7), 2275-2296.

Mufti, A.A. and Bakht, B., 2002. *The benefits of structural health monitoring*. In: Casas, J.R., Frangopol, D.M. and Nowak, A.S. (eds), Proceeding of 1st International Conference on Bridge Maintenance, Safety and Management (IABMAS 2002), Barcelona, Spain:CIMNE

Mukhopadhyay, S., Luş, H. & Betti, R., 2014. Modal parameter based structural identification using input–output data: Minimal instrumentation and global identifiability issues. *Mechanical Systems and Signal Processing*, 45 (2), 283-301.

National Transportation Safety Board, 2008. *Collapse of I-35W Highway Bridge Minneapolis, Minnesota*. Highway Accident Report NTSB/HAR-08/03, Washington, D.C.:NTSB.

Nguyen, K., Freytag, B., Ralbovsky, M. & Rio, O., 2015. Assessment of serviceability limit state of vibrations in the uhpfrc-wild bridge through an updated fem using vehicle-bridge interaction. *Computers & Structures,* 156, 29-41.

Ni, Y., Xia, H., Wong, K. & Ko, J., 2011. In-service condition assessment of bridge deck using long-term monitoring data of strain response. *Journal of Bridge Engineering,* 17 (6), 876-885.

Okasha, N.M. & Frangopol, D.M., 2012. Integration of structural health monitoring in a system performance based life-cycle bridge management framework. *Structure and Infrastructure Engineering,* 8 (11), 999-1016.

Park, J.-H. & Asada, H., 1993. Concurrent design optimization of mechanical structure and control for high speed robotss. *American Control Conference*, IEEE, 2673-2679.

Park, W., Kim, H.-K. & Park, J., 2012. Finite element model updating for a cable-stayed bridge using manual tuning and sensitivity-based optimization. *Structural Engineering International*, 22 (1), 14-19.

Ratay, R.T., 2006. Structural condition assessment—an introduction. *Structures Congress 2006*: Structural Engineering and Public Safety, 1-2.

Robert-Nicoud, Y., Raphael, B., Burdet, O. & Smith, I.F.C., 2005. Model identification of bridges using measurement data. *Computer-Aided Civil and Infrastructure Engineering,* 20 (2), 118-131.

Saad-Eldeen, S., Garbatov, Y. & Soares, C.G., 2014. Strength assessment of a severely corroded box girder subjected to bending moment. *Journal of Constructional Steel Research,* 92, 90-102.

Saitta, S., Kripakaran, P., Raphael, B. & Smith, I.F., 2008. Improving system identification using clustering. *Journal of Computing in Civil Engineering*, 22 (5), 292-302.

Saltelli, A., 2002. Making best use of model evaluations to compute sensitivity indices. *Computer Physics Communications*, 145 (2), 280-297.

Sanayei, M., Khaloo, A., Gul, M. & Catbas, F.N., 2015. Automated finite element model updating of a scale bridge model using measured static and modal test data. *Engineering Structures,* 102, 66-79.

Sanayei, M., Phelps, J.E., Sipple, J.D., Bell, E.S. & Brenner, B.R., 2011. Instrumentation, nondestructive testing, and finite-element model updating for bridge evaluation using strain measurements. *Journal of bridge engineering,* 17 (1), 130-138.

Sartor, R.R., Culmo, M.P. & Dewolf, J.T., 1999. Short-term strain monitoring of bridge structures. *Journal of Bridge Engineering*, 4 (3), 157-164.

Schlune, H. & Plos, M., 2008. *Bridge assessment and maintenance based on finite element structural models and field measurements*. Chalmers University of Technology.

Schlune, H., Plos, M. & Gylltoft, K., 2009. Improved bridge evaluation through finite element model updating using static and dynamic measurements. *Engineering structures,* 31 (7), 1477-1485.

Shahrooz, B., Ho, I., Aktan, A., De Borst, R., Blaauwendraad, J., Van Der Veen, C.,

Iding, R. & Miller, R., 1994. Nonlinear finite element analysis of deteriorated RC slab bridge. *Journal of Structural Engineering*, 120 (2), 422-440.

Shen, Z. & Jensen, W., 2015. Integrated 3d bridge-condition visualization (bcv) to facilitate element-based bridge condition rating (ebcr), Report on NDOR Research Project M004, University of Nebraska-Lincoln, Nebraska.

Simon, P., Goldack, A. & Narasimhan, S., 2016. Mode shape expansion for lively pedestrian bridges through kriging. *Journal of Bridge Engineering,* 21 (6), 04016015.

Song, S.-T., Chai, Y. & Hida, S.E., 2003. Live-load distribution factors for concrete box-girder bridges. *Journal of bridge engineering*, 8 (5), 273-280.

Sousa, H., Bento, J. & Figueiras, J., 2014. Assessment and management of concrete bridges supported by monitoring data-based finite-element modeling. *Journal of Bridge Engineering,* 19 (6), 05014002.

Soyoz, S. & Feng, M.Q., 2009. Long-term monitoring and identification of bridge structural parameters. *Computer-Aided Civil and Infrastructure Engineering*, 24 (2), 82-92.

Tabsh, S.W. & Nowak, A.S., 1991. Reliability of highway girder bridges. *Journal of Structural Engineering*, 117 (8), 2372-2388.

Tarhini, K. & Frederick, G., 1995. Lateral load distribution in i-girder bridges. *Computers & structures,* 54 (2), 351-354.

Taylor, Z., Amini, O. & Van De Lindt, J.W., 2011. *Approach for establishing approximate load carrying capacity for bridges with unknown material and unknown design properties*. Technical Report, Mountain-Plains Consortium & Colorado State University, Colorado. .

Teughels, A. & De Roeck, G., 2003. Damage assessment of the z24 bridge by fe model updating. *Key engineering materials*, 245-246, 19-26.

Veshosky, D., Beidleman, C.R., Buetow, G.W. & Demir, M., 1994. Comparative analysis of bridge superstructure deterioration. *Journal of Structural Engineering,* 120 (7), 2123-2136.

Wan, H.-P. & Ren, W.-X., 2014. Parameter selection in finite-element-model updating by global sensitivity analysis using gaussian process metamodel. *Journal of Structural Engineering,* 141 (6), 04014164.

Wang, M., Heo, G. & Satpathi, D., 1997. Dynamic characterization of a long span bridge: A finite element based approach. *Soil Dynamics and Earthquake Engineering,* 16 (7-8), 503-512.

Xia, P.-Q. & Brownjohn, J.M., 2004. Bridge structural condition assessment using systematically validated finite-element model. *Journal of Bridge Engineering,* 9 (5), 418-423.

Xiao, X., Xu, Y. & Zhu, Q., 2014. Multiscale modeling and model updating of a cable-stayed bridge. Ii: Model updating using natural frequencies and influence lines. *Journal of Bridge Engineering,* 20 (10), 04014113.

Xu, Y.-L., Zhang, X.-H., Zhu, S. & Zhan, S., 2016. Multi-type sensor placement and response reconstruction for structural health monitoring of long-span suspension bridges. *Science bulletin,* 61 (4), 313-329.

Zhang, Q., Chang, T.-Y.P. & Chang, C.C., 2001. Finite-element model updating for the kap shui mun cable-stayed bridge. *Journal of Bridge Engineering*, 6 (4), 285-293.

Zhang, Q., Chang, C.C. & Chang, T.-Y.P., 2000. Finite element model updating for

structures with parametric constraints. *Earthquake engineering & structural dynamics,* 29 (7), 927-944.

Zhu, Q., Xu, Y. & Xiao, X., 2014. Multiscale modeling and model updating of a cable-stayed bridge. I: Modeling and influence line analysis. *Journal of Bridge Engineering,* 20 (10), 04014112.

Ziaei-Rad, S. & Imregun, M., 1996. On the accuracy required of experimental data for finite element model updating. *Journal of Sound and vibration,* 196 (3), 323-336.

Abstract in Korean

운용중인 교량 구조물은 노후화, 극한상황에 따른 피해 등으로 인해 부재의 열화를 겪는다. 즉, 각 부재의 탄성계수, 단면 넓이 등 구조변수값은 설계도면상의 그것과 달라지게 되며 그로 인해 교량의 구조적 성능 또한 지속적으로 변화한다. 이러한 교량을 안전하고 비용효율적으로 유지관리하기 위해서는 구조물의 현재 성능에 대한 정확한 평가가 선행되어야 한다. 최근 교량의 구조 성능을 나타내는 객관적인 지표로서 Load Rating factor(RF)를 사용하는 경우가 증가하고 있다. RF는 구조물의 활하중효과에 대한 내하력의 비율을 수치로 나타낸 것이기 때문에, 다른 방식들에 비해 정량적이고 객관적이라는 점에서 우수성을 보인다. RF를 정확하게 산정하기 위한 한 가지 방법은 유한요소해석을 이용하는 것이다. 이를 위해서는 초기 설계도서에 기반하여 교량의 유한요소모델을 구성한 후, 운용 중 교량의 거동을 계측하여 교량의 현재 상태를 반영하도록 업데이트해야 한다. 일반적으로 유한요소모델 업데이트를 위해서는 차량재하시험을 수행한다. 그로부터 거더의 처짐, 변형률 등 부재 단위 응답을 계측한 후, 수치해석으로부터 얻은 응답과의 오차가 최소화되도록 유한요소모델의 구조변수값을 수정하는 최적화 과정을 거친다. 하지만 이 방법은 공용중인 교량에 대한 전면적인 교통 통제 등 사회/경제적 비용을 크게 요구한다는 단점이 있다. 이에 대한 대안으로 상시진동시험으로부터 얻을 수 있는 고유진동수, 모드형상 등의 동적 응답만으

로 유한요소모델을 업데이트하는 방법도 있다. 하지만 이 방법을 통해 전역적인 거동에 대한 대략적 정보를 얻을 수는 있어도, 부재 단위의 강성정보를 얻는 것은 한계가 있다. 특히 유한요소해석을 통해 RF를 산정할 때에는 부재단위의 정확한 업데이트가 요구되기 때문에, 상시진동데이터를 이용해 업데이트한 모델로는 한계가 있음이 지적되어 왔다.

이 논문은 교량의 거더 간 상대적 처짐 (Relative Girder Displacement, RGD) 개념을 도입하여, 상시진동데이터를 이용한 유한요소모델 업데이트의 정확도를 향상시키는 방안을 제시한다. RGD는 동적 및 정적 하중에 대해 거의 동일한 값을 나타내며 부재단위의 강성 정보를 제공하기 때문에 기존의 한계를 극복할 수 있을 것으로 생각되었다. 그리고 MAC과 유사하게 벡터로서 형상을 표현하는 Relative Girder Displacement Assurance Criterion (RGDAC) 개념을 정의함으로써 개별적인 값으로 표현되는 RGD의 단점을 보완하였다. RGD와 RGDAC를 이용하여 목적함수를 구성하는 방식을 다양화하며 각각이 모델 업데이트에 미치는 영향을 분석함으로써 높은 모델을 얻기 위해 가장 적합한 목적함수 설정 방법을 제안한다. 제안된 방법을 검증하기 위해 실교량에 기반한 가상 교량모델을 구성하고 모델 업데이트를 수행했다. 임의의 부재에 대해 강성의 저하를 가정하고, 다양한 목적함수를 설정해 업데이트한 결과 제안하는 방법의 우수함을 보일 수 있었다. 또한 하중의 위치를 달리하여 업데이트효과를 검증함으로써 제안된 방법의 일반성을 확인하였다.

적용성을 보이기 위한 예제로서 실험 데이터를 이용한 실교량의 유한요소모델 업데이트를 수행했다. 또 업데이트된 모델을 이용하여 RF를 산정함으로써 제안된 방법의 실제적인 활용을 보여주었다.

주요어: 유한요소모델 업데이트, 상시진동데이터, Relative Girder Displacement (RGD), Relative Girder Displacement Assurance Criterion (RGDAC)

학 번: 2011－23392